SEMICLASSICAL DESCRIPTION OF NUCLEAR BULK PROPERTIES

Matthias Brack
Institut für Theoretische Physik
Universität Regensburg
D-8400 Regensburg, W. Germany

1. INTRODUCTION

In these lectures we shall discuss the use of density functionals for calculating static nuclear bulk properties such as average binding energies, density distributions and their moments, and deformation energies.

The idea of expressing the total energy of a nucleus as a functional of the local density $\rho(r)$ and to formulate with it a variational principle

$$\frac{\delta}{\delta\rho}\int d^3r\left\{\mathcal{E}[\rho(\vec{r})]-\lambda\rho(\vec{r})\right\} = 0 \qquad (1.1)$$

has been used as early in the history of nuclear physics as 50 years ago, namely in the pioneering work which led to the famous semi-empirical Bethe-Weizsäcker mass formula.[1,2] Sophistication of the energy density functional $\mathcal{E}[\rho]$ was developed along with the understanding of the nuclear force[3-5] and led to the so-called energy density formalism.[6,7] The theoretical justification of the variational approach eq. (1.1) came from outside nuclear physics in form of the now well-known theorem by Hohenberg and Kohn.[8]

Whereas the main difficulty of density functional calculations in solid state physics and quantum chemistry lies in the development of sufficiently accurate exchange and correlation energy functionals, their applications in nuclear physics are further strongly handicapped by the fact that the basic nucleon-nucleon interaction is only partially known and, due to its repulsive core, cannot be used directly in a perturbation expansion. We refer to the literature for comprehensive discussions of our present knowledge of the

nucleon-nucleon interaction[9] and its use in Brückner theory[10,11] calculations for nuclear matter and finite nuclei.[12,13]

The energy density variational calculations performed until the late sixties, in which mostly the Brückner G-matrix in the local density approximation[11,12] was used, have been reviewed by Lombard.[7] Typically, the experimental binding energies of spherical nuclei could be reproduced to within $\sim$ (1-10) MeV and their radii within $\sim$ (1-4) %. (The shell effects, which cannot be included in this formalism, contribute about $\pm$ (1-15) MeV to the total energy and less than 1 % to the radii.) The density profiles obtained with these calculations were as a rule rather poor. This deficiency can be traced back mainly to the use of an insufficient kinetic energy density functional: mostly, the Thomas-Fermi relation $\tau = \kappa\rho^{5/3}$ was used, sometimes a gradient correction with adjustable coefficients was added. The corresponding large errors in the kinetic energies were partially made up by readjustments of the nuclear force parameters, but this could not help to improve the resulting density profiles.

Several recent developments which took place over the last 10-15 years allow to reassess now the energy density formalism in a much more rigorous and quantitative way.[15,16] The developments are the following:

1. Phenomenological effective nucleon-nucleon interactions, which may be understood as mathematically simple parametrisations of a density-dependent effective G-matrix, can be constructed and used in the Hartree-Fock (HF) approximation to reproduce surprisingly well nuclear ground-state energies, densities, radii, deformation energies (in particular also fission barriers of heavy nuclei[15,16]) and some properties of highly collective excitations such as the nuclear giant resonances.[17,18] (See ref. 19 for a review of such effective forces and their applications in HF (plus RPA) calculations.) In particular, the Skyrme type effective interactions [3,20] allow to write the nuclear part of the HF energy as a functional of local one-body densities only, which makes them especially well-suited for the use in density functional methods.
2. The Strutinsky method[21] not only proved to be an efficient phenomenological tool for fission barrier calculations (see, e.g.ref.22), but it also provides a quantitative way[23] to extract an average part of the HF energy which is semiclassical in its nature and can be calculated by density functional methods. This allows to avoid the very difficult problem of describing the shell effects by density functionals; it was demonstrated[15,23] that the shell

effects can be included perturbatively at the end of a self-consistent semiclassical calculation without any significant loss of accuracy compared to an exact HF calculation.

3. The extended Thomas-Fermi (ETF) model, based on a semiclassical $\hbar$ expansion of the partition function or the Bloch density,[24] was reintroduced into nuclear physics[25,26] and successfully used to calculate the average energy of nucleons in realistic potentials.[27] It was, in particular, also shown[26-28] that this average energy is identical to that obtained with the microscopical Strutinsky averaging method. From the same ETF model, density gradient expansions of the kinetic energy density functional $\tau[\rho]$ and a spin-orbit density functional $\vec{J}[\rho]$ can be derived; they have recently been extended to include contributions from nonlocalities of the average nuclear potential such as variable effective nucleon masses and spin-orbit potentials.[29,30] The ETF functional for $\tau[\rho]$ was furthermore demonstrated in microscopical test calculations[29,30] to reproduce very accurately the average kinetic energy of finite nuclei.

The strategy of the density functional method discussed in these lectures is thus the following: We use effective Skyrme type forces, as they are determined in HF calculations, without touching their parameters. We then use the density functionals $\tau[\rho]$ and $\vec{J}[\rho]$ determined from the ETF model once for all, without readjusting any of their coefficients, in variational calculations for the average nuclear properties of interest. In this way, the semiclassical reslts can at any time be tested against microscopically averaged HF results and possible deficiencies of the density functionals can be disentangled from possible deficiencies of the Skyrme forces themselves. The shell effects, wherever they are of importance, are added perturbatively at the end of the semiclassical variational calculation in terms of the corresponding average mean fields.

These lectures will be structured as follows: In section 2 we discuss in some more detail the above mentioned newer developments, in order to provide the basic justification of the semiclassical variational method. In section 3, we shall present - after a discussion of the ETF-Euler variational equations - the results for static nuclear bulk properties obtained in semiclassical calculations with a restricted, but flexible variational space of trial nuclear densities. We shall also shortly discuss there the expansion of the semiclassical nuclear binding energies in a liquid drop model (LDM) type series, which allows to link the phenomenological LDM or droplet model parameters back to those of the Skyrme force. In section 4, we shall finally discuss some extensions of the semiclassical density functional method.

2. FOUNDATION OF THE SEMICLASSICAL VARIATIONAL METHOD FROM THE SKYRME-HF FORMALISM

2.1. The Skyrme-HF Energy Density

We shall briefly outline here the structure of the energy density obtained with effective forces of the Skyrme type.[3] They have mathematically a zero range; however, velocity dependent terms mock up the finite (but short) range of the nuclear force. This allows to write the nuclear part of the HF energy as a functional of local one-body densities only. Correspondingly, the total HF energy is written in the form

$$E_{HF} = \int d^3r \, [\mathcal{E}_{Sky}(\vec{r}) + \mathcal{E}_{Coul}(\vec{r})] \, . \tag{2.1}$$

The nuclear (Skyrme) part

$$\mathcal{E}_{Sky}(\vec{r}) = \mathcal{E}_{Sky}[\rho_q(\vec{r}), \tau_q(\vec{r}), \vec{J}_q(\vec{r})] \tag{2.2}$$

is a simple functional of the local nucleon densities $\rho_q(\vec{r})$, kinetic energy densities $\tau_q(\vec{r})$ and spin-orbit densities $\vec{J}_q(\vec{r})$ ($q = n, p$ for neutrons and protons, respectively) defined by

$$\rho_q(\vec{r}) = \sum_{\nu,s} |\varphi_\nu(\vec{r},s,q)|^2 \, n_\nu^q \, , \tag{2.3}$$

$$\tau_q(\vec{r}) = \sum_{\nu,s} |\vec{\nabla} \varphi_\nu(\vec{r},s,q)|^2 \, n_\nu^q \, , \tag{2.4}$$

$$\vec{J}_q(\vec{r}) = (-i) \sum_{\nu,s,s'} \varphi_\nu^*(\vec{r},s',q) \, \vec{\nabla} \varphi_\nu(\vec{r},s,q) \times \langle s'|\vec{\sigma}|s\rangle \, n_\nu^q \, , \tag{2.5}$$

where $\varphi_\nu(\vec{r},s,q)$ are the single-particle wave functions with orbital and spin quantum numbers ν and s, respectively, and n_ν^q are the occupation numbers (equal to 1 or 0 in the pure HF case, or v_ν^2 if pairing correlations are included in the BCS approximation[32]). The Coulomb energy density is the sum of the direct term and the exchange term, the latter taken in the well-known Slater approximation which has proved sufficiently accurate for all practical purposes[33]:

$$\mathcal{E}_{Coul}(\vec{r}) = e^2 \rho_p(\vec{r}) \frac{1}{2} \int d^3\vec{r}' \, \frac{\rho_p(\vec{r}')}{|\vec{r} - \vec{r}'|} - \frac{3}{4} e^2 \left(\frac{3}{\pi}\right)^{1/3} \rho_p^{4/3}(\vec{r}) \, . \tag{2.6}$$

We refer to the original paper of Vautherin and Brink[20] for the derivation and the exact form of the functional $\mathcal{E}_{Sky}(\vec{r})$. (For the extended form of Skyrme forces where the density dependent term contains a variable power of ρ, see e.g. ref. 34.)

As an illustration we give here the expression of $\mathcal{E}_{Sky}(\vec{r})$ for the case of a symmetric nucleus with $\rho_n = \rho_p = \rho/2$ etc.:

$$\mathcal{E}_{Sky}(\vec{r}) = \frac{\hbar^2}{2m}\tau + \frac{3}{8}t_0\rho^2 + \frac{1}{16}(3t_1+5t_2)\tau\rho + \frac{1}{16}t_3\rho^{2+\alpha} + \frac{1}{64}(9t_1-5t_2)(\vec{\nabla}\rho)^2 + \frac{3}{4}W_0\,\vec{J}\cdot\vec{\nabla}\rho. \tag{2.7}$$

The HF equations, obtained by varying the wave functions $\varphi_\nu^q = \varphi_\nu(\vec{r},s,q)$, take the form of Schrödinger equations with variable effective nucleon masses and spin-orbit potentials:

$$\hat{H}^q_{HF}\varphi^q_\nu = \left[-\vec{\nabla}\cdot\frac{\hbar^2}{2m^*_q(\vec{r})}\vec{\nabla} + V_q(\vec{r}) - i\vec{W}_q(\vec{r})\cdot(\vec{\nabla}\times\vec{\sigma})\right]\varphi^q_\nu = \varepsilon^q_\nu\varphi^q_\nu \,. \tag{2.8}$$

The local potentials $V_q(\vec{r})$, effective masses $m^*_q(\vec{r})$ and spin-orbit potentials $\vec{W}_q(\vec{r})$ are given by the relations

$$V_q(\vec{r}) = \frac{\delta\mathcal{E}(\vec{r})}{\delta\rho_q(\vec{r})} \equiv \frac{\partial\mathcal{E}}{\partial\rho_q} - \vec{\nabla}\cdot\frac{\partial\mathcal{E}}{\partial(\vec{\nabla}\rho_q)} + \Delta\frac{\partial\mathcal{E}}{\partial(\Delta\rho_q)}\,, \tag{2.9}$$

$$\frac{\hbar^2}{2m^*_q(\vec{r})} = \frac{\partial\mathcal{E}(\vec{r})}{\partial\tau_q(\vec{r})}\,, \tag{2.10}$$

$$\vec{W}_q(\vec{r}) = \frac{\partial\mathcal{E}(\vec{r})}{\partial\vec{J}_q(\vec{r})}\,. \tag{2.11}$$

where $\mathcal{E}(\vec{r})$ is the sum of the nuclear and the Coulomb energy density.

Usually, the force parameters $t_0, t_1, t_2, t_3, \alpha$ etc. are determined by fits of experimental groundstate properties of a series of (mostly spherical) nuclei. However, most of them are related to each other, and restricted in their range of values, by imposing the more or less well established saturation properties of infinite nuclear matter, such as the binding energy per nucleon E/A (i.e the volume energy of the mass formula), the saturation density ρ_∞, the effective mass m^*_∞ or the nuclear matter incompressibility K_∞. Imposing their empirical values, the choice of the force parameters

is greatly restricted, although still innumberable parameter sets can be found in the literature.[19,35] The parameter α of the density dependent term in the Skyrme functional eq. (2.7) is rather strongly restricted by the values of K_∞ and m^*_∞. In fact, if values in the ranges

$$\begin{aligned} 210\ \text{MeV} \lesssim K_\infty &\lesssim 240\ \text{MeV} \\ 0.7 \lesssim m^*_\infty/m &\lesssim 0.8 \end{aligned} \tag{2.12}$$

are imposed, as they are required in order to fit the giant monopole and quadrupole resonances by RPA calculations,[17,18] one finds that α must be of the order

$$1/6 \lesssim \alpha \lesssim 1/3\ . \tag{2.13}$$

Having imposed "reasonable" nuclear matter properties alone guarantees, of course, in no way that a force will have good surface properties of finite nuclei, which then are adjusted by actual HF calculations and fits to experimental data. Even more it must be considered a great success that good fits to many data were obtained, considering the fact that the nuclear matter properties fix already five combinations of the typically 7-8 Skyrme parameters. For detailed comparisons of HF (+BCS) results to experimental data, we can only refer here to the abundant literature.[17-19,35-37]

It might be worth spending a few words on the nature of this HF + Skyrme formalism. Although it formally is a Hartree-Fock procedure, it may well go beyond this framework what the physics is concerned. Due to the fact that the Skyrme force is a parametrized G-matrix (and can be derived qualitatively from a Brückner G-matrix[13]), short-range correlations are built into it from the very beginning. But also long-range correlations can be contained in what above is called the HF energy, because the HF equations (2.8) can be understood as Kohn-Sham equations,[38] generalized to include nonlocal parts of the potential. Noting that, in fact, the mean fields in eq. (2.8) are nothing but functional derivatives of a parametrized energy density, one recognizes that due to the Hohenberg-Kohn theorem[8] all kinds of correlation energies may be contained in the energy E_{HF} eq. (2.1)

2.2 Separation of Shell Effects

The direct application of the Skyrme energy functional eq. (2.2) to the density variational method is handicapped by the presence of the kinetic energy and spin-orbit densities $\tau_q(\vec{r})$ and $\vec{J}_q(\vec{r})$. In principle, we know from the Hohenberg-Kohn theorem[8] that there exist unique functionals $\tau[\rho]$ and $\vec{J}[\rho]$ which allow to express these densities

in terms of the local nucleon densities $\rho_q(\vec{r})$. However we do not know these functionals and there is little chance to determine them exactly. They certainly must be nonlocal, since the shell effects contained in $\tau_q(\vec{r})$ and $\vec{J}_q(\vec{r})$ are not local, but global properties of the nucleus.[39,40]

This problem can be overcome by averaging out the shell effects and expressing the average of the energy by a functional of the average densities $\rho_q(r)$. This can be justified by means of Strutinsky's energy averaging method[21] which, in fact, allows to decompose the exact HF energy in a rather unique way into an average and a fluctuating ("shell-correction") part[21-23]:

$$E_{HF} \simeq \tilde{E}_{HF} + \delta_1 E_n + \delta_1 E_p \quad . \tag{2.14}$$

Hereby the average energy E_{HF} is practically calculated in the same way as the exact energy E_{HF} through eqs. (2.1) - (2.6), but replacing the quantum mechanical densities eqs. (2.3) - (2.5) by the averaged densities obtained by means of the Strutinsky averaging occupation numbers $\tilde{n}^q_\nu$,[22,28]

$$\tilde{\varrho}_q(\vec{r}) = \sum_{\nu,s} |\varphi_\nu(\vec{r},s,q)|^2 \, \tilde{n}^q_\nu \quad , \tag{2.15}$$

etc. The shell-correction energy $\delta_1 E_q$ in eq. (2.14) is defined by

$$\delta_1 E_q = \sum_\nu \hat{\varepsilon}^q_\nu (n^q_\nu - \tilde{n}^q_\nu) \quad , \tag{2.16}$$

where $\hat{\varepsilon}^q_\nu$ are the eigenvalues of the average HF Hamiltonians $\tilde{H}^q_{HF}$ defined through eqs. (2.8) - (2.11) in terms of the averaged densities, i.e.

$$\tilde{H}^q_{HF} \hat{\varphi}^q_\nu = \hat{H}_{HF}[\tilde{\varrho}_q, \tilde{\tau}_q, \tilde{\vec{J}}_q] \hat{\varphi}^q_\nu = \hat{\varepsilon}^q_\nu \hat{\varphi}^q_\nu \quad . \tag{2.17}$$

Formally, eq. (2.14) just represents the lowest two terms of a Taylor expansion of the HF energy around the average parts of the densities. (See ref. 23 for a discussion and further literature on this subject.) In extended numerical calculations[23] it has been checked that the missing higher order terms in eq. (2.14) are negligible for all practical purposes. In particular if the averaging by means of the $\tilde{n}^q_\nu$ is done selfconsistently (see also the next subsection), the two sides of eq. (2.14) are equal to within less than $\sim$ 0.5 MeV even in heavy, strongly deformed nuclei (corresponding to an ccuracy of better than 10^{-3}).

Two important conclusions could be drawn from these numerical results[23]:

1) The averaged HF energy $\tilde{E}_{HF}$ has all the properties of a LDM type, semiclassical energy.
2) The selfconsistency is only important for the average quantities ($\tilde{E}_{HF}$, $\tilde{H}^q_{HF}$, $\tilde{\rho}_q$, etc); the shell effects can, in fact, be added perturbatively.

This provides us with a strong motivation to replace the above sketched microscopical selfconsistent calculations of $\tilde{E}_{HF}$ by a semiclassical calculation. For its realization, it was important to quantitatively secure the equivalence of the Strutinsky averaging procedure with a semiclassical expansion of the energy, as will be discussed in the following subsection.

2.3 Strutinsky Averaging as a Microscopical Link to the ETF Model

Strutinsky[21] and Tyapin[41] surmised that the numerically Strutinsky-averaged energies not only correspond to those obtained in the Fermi gas theory, but that they contain also inhomogeneity corrections such as they are obtained in the so-called extended Thomas-Fermi (ETF) model.[42]

Bhaduri and Ross[25] proposed to calculate the average energy of nucleons in various model potentials by employing a $\hbar$-expansion of the partition function, which actually had been developed long ago by Wigner and Kirkwood,[24] and demonstrated the closeness of their results to those of a numerical Strutinsky averaging. (We shall discuss the Wigner-Kirkwood expansion and the ETF relations derived from it in section 2.4.) For harmonic oscillator potentials, the exact equivalence of the Strutinsky averaging method and the semiclassical $\hbar$-expansion was proved analytically.[26,28] For realistic, deformed Woods-Saxon type potentials including spin orbit fields, the two methods were shown numerically[27] to yield identical energies to within $\sim$ 1 - 1.5 MeV (out of several GeV), which is roughly the uncertainty in either method.

It is thus well established that - at least as energies are concerned and with the numerical accuracy practically required - the microscopical Strutinsky averaging procedure is equivalent to a semiclassical $\hbar$-expansion. Therefore it seems natural to use the ETF functionals $\tau[\rho]$ and $\vec{J}[\rho]$ obtained from the same $\hbar$-expansion (see next section) in order to calculate the average HF energy $\tilde{E}_{HF}$ in a semiclassical, and thus much more economical way.

That the energy $\tilde{E}_{HF}$ - which was obtained microscopically in ref. 23, as explained in sect 2.2 - can be expressed as a functional of the average densities $\tilde{\rho}_q(\vec{r})$ eq. (2.15) is again a consequence of the Hohenberg-Kohn theorem. The iterative inclusion of the Strutinsky occupation numbers $\tilde{n}^q_\nu$ in the HF cycle has, in fact, been

formulated in a strictly variational way,[23] including a proper constraint in the energy to be made stationary (and found to be minimized in actual calculations). The Hohenberg-Kohn theorem[8] applies therefore to this variational averaged system as well as it applies to any variational system of Fermions interacting through a 2-body force.

2.4 The ETF Model and its Density Functionals

We shall in the following sketch the semiclassical $\hbar$-expansion developed by Wigner and Kirkwood,[24] which provides a convenient tool to derive the ETF functionals $\tau[\rho]$ and $\vec{J}[\rho]$ which we are interested in. For the sake of a simple notation, we shall presently restrict ourselves to the case of N nucleons (one kind only) in a given local (HF) potential $V(\vec{r})$. Let φ_ν and ε_ν be the eigenfunctions and eigenvalues of the corresponding Schrödinger equation:

$$\hat{H}\varphi_\nu = [\hat{T} + V(\vec{r})]\varphi_\nu = \varepsilon_\nu \varphi_\nu \quad . \tag{2.18}$$

Next we define the Bloch density matrix

$$C(\vec{r},\vec{r}';\beta) = \sum_\nu \varphi_\nu^*(\vec{r}')\varphi_\nu(\vec{r})e^{-\beta\varepsilon_\nu} \quad , \tag{2.19}$$

where the sum goes over the complete spectrum (including an integral over the continuum, if present). From C, we obtain by an inverse Laplace transform the usual density matrix

$$\begin{aligned} \rho(\vec{r},\vec{r}') &= L_\lambda^{-1}\left[\frac{1}{\beta}C(\vec{r},\vec{r}';\beta)\right] \\ &= \frac{1}{2\pi i}\int_{c-i\infty}^{c+i\infty} d\beta e^{\lambda\beta}\frac{1}{\beta}C(\vec{r},\vec{r}';\beta) \quad , \end{aligned} \tag{2.20}$$

from which in turn, the local densities $\rho(\vec{r})$ and $\tau(\vec{r})$ can be determined

$$\rho(\vec{r}) = \sum_{\nu=1}^{N} |\varphi_\nu(\vec{r})|^2 = \rho(\vec{r},\vec{r}') \quad , \tag{2.21}$$

$$\tau(\vec{r}) = \sum_{\nu=1}^{N} |\vec{\nabla}\varphi_\nu(\vec{r})|^2 = \vec{\nabla}_r \cdot \vec{\nabla}_{r'} \rho(\vec{r},\vec{r}')\big|_{\vec{r}=\vec{r}'} \quad . \tag{2.22}$$

In eq. (2.20), λ is the Fermi energy which is fixed by the particle number conservation

$$\int \rho(\vec{r}) d^3r = N \quad . \tag{2.23}$$

The idea of Wigner and Kirkwood was to expand $C(\vec{r},\vec{r}';\beta)$ around its value obtained in the Thomas-Fermi approximation:

$$C_{TF}(\vec{r},\vec{r}';\beta) = \left(\frac{m}{2\pi\hbar^2\beta}\right)^{3/2} e^{-\beta V\left(\frac{\vec{r}+\vec{r}'}{2}\right)} e^{-\frac{m}{2\hbar^2\beta}(\vec{r}-\vec{r}')^2} \tag{2.24}$$

One makes the ansatz

$$C(\vec{r},\vec{r}';\beta) = C_{TF}(\vec{r},\vec{r}';\beta) \times \{1 + \hbar\chi_1 + \hbar^2\chi_2 + \ldots\} \ , \tag{2.25}$$

thus expanding the ratio of the exact to the TF Bloch function in powers of $\hbar$. The χ_n are functions of $\vec{r},\vec{r}'$ and β which contain combinations of n gradients acting on $V(\vec{r})$. Uhlenbeck and Beth[42] worked out a recursive scheme to obtain the χ_n successively (see also ref. 43). By Laplace-inverting the series eq. (2.25) back term by term, one obtains an expansion of the density matrix eq. (2.20) and thus of $\rho(\vec{r})$ and $\tau(\vec{r})$, to which only even powers of $\hbar$ (i.e. χ_n with even n) contribute. We quote here the results up to order $\hbar^2$

$$\rho_{ETF}(\vec{r}) = \frac{1}{3\pi^2}\left(\frac{2m}{\hbar^2}\right)^{3/2}(\lambda - V(\vec{r}))^{3/2} \times \Theta(\lambda - V(\vec{r})) \times \tag{2.26}$$

$$\times \left\{1 - \frac{1}{8}\frac{\hbar^2}{2m}\left[\Delta V(\lambda - V)^{-2} + \frac{1}{4}(\vec{\nabla} V)^2(\lambda - V)^{-3}\right]\right\} \ ,$$

$$\tau_{ETF}(\vec{r}) = \frac{1}{5\pi^2}\left(\frac{2m}{\hbar^2}\right)^{5/2}(\lambda - V(\vec{r}))^{5/2} \times \Theta(\lambda - V(\vec{r})) \times \tag{2.27}$$

$$\times \left\{1 - \frac{5}{8}\frac{\hbar^2}{2m}\left[\frac{5}{3}\Delta V(\lambda - V)^{-2} - \frac{3}{4}(\vec{\nabla} V)^2(\lambda - V)^{-3}\right]\right\} \ .$$

In the lowest order terms we recognize the TF expressions; the $\hbar^2$-corrections lead to the well-known divergencies at the classical turning points $\vec{r}_\lambda$ given by $\lambda = V(\vec{r}_\lambda)$. (Due to the step functions, both densities are identically zero outside the classically allowed region.)

In spite of their turning point divergencies, the densities eqs. (2.26), (2.27) can be shown[43] to lead to finite energies and particle numbers, even if the $\hbar^4$ terms are included. This shows that the ETF densities are rather to be understood as distributions with well-defined integrals and moments (see also ref. 44). The energies so obtained form a rapidly converging asymptotic series

$$E_{ETF} = E_{TF} + E_2 + E_4 + \ldots \tag{2.28}$$

The sum of the first three terms (i.e. up to order $\hbar^4$) converges typically to within $\sim$ 1 MeV and agrees, as mentioned in section 2.3 above, with the energy obtained by Strutinsky averaging:

$$E_{ETF} \simeq \tilde{E}_{Str} = \sum_\nu \varepsilon_\nu \tilde{n}_\nu \, . \tag{2.29}$$

We shall not discuss here the technicalities of including effective mass and spin-orbit contributions, which can be done starting from a Hamiltonian of Skyrme type eq. (2.8); they can be found in the literature.[27,43]

Before coming to the construction of the ETF density functionals, we mention that a way of removing the turning point divergencies in $\rho_{ETF}(\vec{r})$ and $\tau_{ETF}(\vec{r})$ by partially resumming the Wigner-Kirkwood series eq. (2.25) will be discussed in sect. 4.2 below.

2.4. a) The functional $\tau[\rho]$ for a local potential

From eqs. (2.26) and (2.27) it is possible to eliminate algebraically the Fermi energy λ, the potential $V(\vec{r})$ and its derivatives, hereby consistently retaining all terms of order $\hbar^2$ and neglecting those of higher orders in $\hbar$. The result is (for one kind of nucleons)

$$\tau[\rho] = \tau_{TF}[\rho] + \tau_2[\rho] \tag{2.30}$$

with the well-known Thomas-Fermi relation

$$\tau_{TF}[\rho] = \kappa \rho^{5/3}, \qquad \kappa = \frac{3}{5}(3\pi^2)^{2/3} \tag{2.31}$$

and the second order gradient correction

$$\tau_2[\rho] = \frac{1}{36}\frac{(\vec{\nabla}\rho)^2}{\rho} + \frac{1}{3}\Delta\rho \quad . \tag{2.32}$$

The first term in $\tau_2[\rho]$ is the so-called Weizsäcker correction; this author[1] derived it in a somewhat ad hoc manner and obtained it with a 9 times larger coefficient. This coefficient has subsequently given rise to a lot of discussion.[4] By now it is clear that various alternative semiclassical expansion procedures[30,41,42] lead to exactly the same relations and coefficients. (For a recent review in which these alternative expansions are discussed and related, see ref. 45.) The coefficient 1/36 of the Weizsäcker term is thus well established in the framework of semiclassical expansions (and for smooth potentials $V(\vec{r})$). The second term in eq. (2.32) does not contribute to the integrated kinetic energy and has therefore often been ignored; it does however contribute to the total Skyrme energy through the terms containing $\tau\rho$, see eq. (2.7).

Going up to order $\hbar^4$ in the expansion of ρ_{ETF} and τ_{ETF} and proceeding in the same way, one obtains the next correction $\tau_4[\rho]$ to the functional, containing up to fourth derivatives of ρ. The somewhat lengthy expression for $\tau_4[\rho]$ is given in refs.[29,31]. When integrating over the whole space, the fourth and third derivatives of ρ can be eliminated by partial integration, and the expression simplifies to

$$\int\tau_4[\rho]d^3r = \frac{1}{6480}(3\pi^2)^{-2/3}\int\rho^{1/3}\left[8\left(\frac{\vec{\nabla}\rho}{\rho}\right)^4 - 27\left(\frac{\vec{\nabla}\rho}{\rho}\right)^2\frac{\Delta\rho}{\rho} + \right. \tag{2.33}$$

Similarly, one obtains

$$\left. + 24\left(\frac{\Delta\rho}{\rho}\right)^2\right]d^3r.$$

$$\int\rho\tau_4[\rho]d^3r = \frac{1}{3240}(3\pi^2)^{-2/3}\int\rho^{4/3}\left[-7\left(\frac{\vec{\nabla}\rho}{\rho}\right)^4 - \right. \tag{2.34}$$

$$\left. - 3\left(\frac{\vec{\nabla}\rho}{\rho}\right)^2\frac{\Delta\rho}{\rho} + 30\left(\frac{\Delta\rho}{\rho}\right)^2\right]d^3r.$$

This procedure can in principle be continued ad libitum, including higher and higher gradient corrections. However, the terms $\tau_n[\rho]$ with $n \geq 6$ diverge for densities which decay exponentially in the tail region. Therefore, the terms up to fourth order must be considered as the converging part of an asymptotic series for $\tau[\rho]$; we shall denote this part by $\tau_{ETF}[\rho]$:

$$\tau_{ETF}[\rho] = \tau_{TF}[\rho] + \tau_2[\rho] + \tau_4[\rho] \quad . \tag{2.35}$$

The above derivation of the functional $\tau_{ETF}[\rho]$ is strictly

speaking not allowed at the classical turning points, where $\tau_{ETF}(\vec{r})$ and $\rho_{ETF}(\vec{r})$ are singular. It holds, however, at any other point. (In the classically forbidden region, $\tau_{ETF}[\rho]$ holds trivially since τ_{ETF} and ρ_{ETF} there are identically zero!) One may therefore hope to be able to use $\tau_{ETF}[\rho]$ everywhere in space by analytical continuation.

The functional $\tau_{ETF}[\rho]$ given by eqs. (2.31)-(2.35) has been tested numerically with the help of microscopically Strutinsky averaged densities $\tilde{\rho}(\vec{r})$ and $\tilde{\tau}(\vec{r})$, defined as in eq. (2.15), for different spherical and deformed potentials.[29,31] The results of these tests may be summarized as follows (for a more detailed discussion, see ref. 31):

1) The functional $\tau_{ETF}[\rho]$ eq. (2.35) reproduces the total Strutinsky averaged kinetic energy within less than $\sim$ 1.5 MeV, corresponding to a few parts in 10^4 for heavy nuclei. This holds independently of the radial shape of the potential, of its deformation and of the particle number, as it should be expected from the Hohenberg-Kohn theorem.
2) The functional also reproduces the integral $G\int\rho\tau d^3r$, as it occurs in the Skyrme energy, within less than 1 MeV (using realistic Skyrme parameters to determine G).
3) The terms due to $\tau_4[\rho]$ are essential for obtaining the correct deformation energies, in particular the fission barriers.

The points 1 and 3 are illustrated in figure 1 (taken from ref.31). It shows the kinetic energy for 112 particles in a deformed harmonic oscillator potential as a function of the deformation parameter $q = \omega_\perp/\omega_z$ which measures the frequency ratio. The different curves are obtained in terms of the Strutinsky averaged density $\tilde{\rho}(\vec{r})$ eq. (2.15) through the ETF functional eq. (2.35)

$$\tilde{T}_n[\tilde{\rho}] = \frac{\hbar^2}{2m}\int d^3r\ \tau\ [\tilde{\rho}(\vec{r})] \quad , \tag{2.36}$$

whereby the index n shows where the functional (2.35) has been truncated (e.g. n = 2 means TF plus 2nd order gradients included). The reference quantity of the test is the microscopically Strutinsky averaged kinetic energy $\tilde{T}$ defined by

$$\tilde{T} = \frac{\hbar^2}{2m}\int\tilde{\tau}(\vec{r})\,d^3r \quad , \tag{2.37}$$

whereby $\tilde{\tau}(\vec{r})$ has been averaged analogously to $\tilde{\rho}(\vec{r})$ eq. (2.15). It is seen that the full functional $\tau_{ETF}[\rho]$ up to 4th order reproduces the energy $\tilde{T}$ exactly within the accuracy of the drawing; the energies

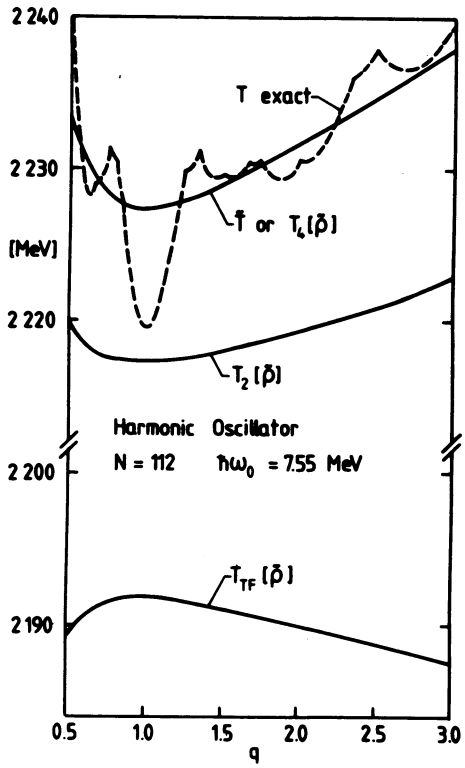

Fig. 1. Kinetic energy of 112 particles in axially deformed harmonic oscillator potential with frequency ratio $q = \omega_1/\omega_2$, obtained with the ETF functional $\tau[\rho]$ up to various orders of gradient corrections (see text). $\widetilde{T}$ is the microscopically Strutinsky-averaged kinetic energy; the dashed curve shows the exact kinetic energy T which includes shell fluctuations.

$\widetilde{T}$ and $T_4[\tilde{\rho}]$ agree in fact within less than 0.1 MeV at all deformations. The 4th order terms $\tau_4[\rho]$ still contribute 10 - 15 MeV to the total kinetic energy and are seen to be important for obtaining the correct deformation dependence. Fig. 1 also contains the exact kinetic energy T (shown by a dashed curve) which contains shell effects. It would of course be hopeless to try to reproduce this exact energy by a local gradient expanded functional, even if the exact quantum mechanical density $\rho(\vec{r})$ is put into the functional $\tau_{ETF}[\rho]$.[31]

We might add here some remarks concerning simplified functionals $\tau[\rho]$ of the form

$$\tau[\rho] = \kappa\rho^{5/3} + \eta\frac{1}{36}\frac{(\vec{\nabla}\rho)^2}{\rho} \tag{2.38}$$

with an adjustable coefficient η, as they have repeatedly been used in the literature.[4,46-48] It may be hoped, indeed, to mock up the 4th order terms $\tau_4[\rho]$ by choosing $\eta > 1$ such as to fit the functional eq. (2.38) to the correct total kinetic energy. However, it is not obvious, then, that the same value of η can be used for all potentials, all deformations and all particle numbers.

In order to illustrate this, we have calculated the quantity

$$\eta = \frac{\int d^3r\,\{\tau_2[\tilde{\rho}] + \tau_4[\tilde{\rho}]\}}{\int d^3r\,\tau_2[\tilde{\rho}]} \tag{2.39}$$

from the results obtained in ref. 31 for the harmonic oscillator potential. In figure 2, the number η eq. (2.39) is plotted against the particle number N (crosses) and against the deformation parameter q (circles). It is seen to be rather constant with values $\eta \simeq 1.4 - 1.5$ for not too small particle numbers. Similar values are also obtained for a deformed Woods-Saxon potential. The value $\eta \simeq 1.4 - 1.5$ is, however, about three times smaller than what typically has been used[46-48]; the reasons for this will be discussed in sect. 3.1 below.

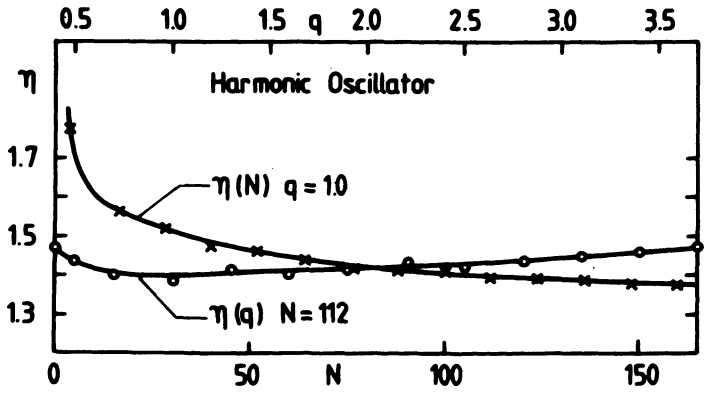

Fig. 2. The parameter η eq. (2.39) obtained for deformed harmonic oscillator potentials is plotted against particle number N (crosses, values on lower axis; evaluated for q = 1) and against deformation q (circles, values on upper axis, evaluated for N = 112 particles).

This result should be used with caution. We cannot expect this procedure of mocking up the 4th order contributions by a single parameter to work for nonlocal potentials. (Indeed, η is dependent on the effective mass of the force.[46]) Furthermore, problems arise with the surface of the densities, if such adjusted functionals as eq. (2.38) are used in variational calculations (see sect. 3.1).

2.4.b) The functionals $\tau[\rho]$ and $\vec{J}[\rho]$ for Skyrme-type nonlocal potentials

For velocity-dependent Skyrme forces, one has to generalize the functional $\tau_{ETF}[\rho]$, since it receives explicit contributions from the nonlocal parts of the HF-potential. Rewriting the Skyrme-HF Hamiltonian (see eq. (2.8)) in the form

$$H_{Sky} = -\frac{\hbar^2}{2m}\vec{\nabla}\cdot f(\vec{r})\vec{\nabla} + V(\vec{r}) - i\vec{W}(\vec{r})\cdot(\vec{\nabla}\times\vec{\sigma}) , \tag{2.40}$$

where $f(\vec{r}) = m/m^*(\vec{r})$, the Wigner-Kirkwood expansion eq. (2.25) can be readily obtained. (The Bloch density C is in this case a 2 x 2 matrix, the χ_n with $n > 1$ containing the Pauli matrices σ_i.) The second-order contribution to the kinetic energy density functional then becomes

$$\tau_2[\rho] = \frac{1}{36}\frac{(\vec{\nabla}\rho)^2}{\rho} + \frac{1}{3}\Delta\rho + \frac{1}{6}\frac{(\vec{\nabla}\rho\cdot\vec{\nabla}f)}{f} + \frac{1}{6}\rho\frac{\Delta f}{f} - \frac{1}{12}\rho\left(\frac{\vec{\nabla}f}{f}\right)^2 + \frac{1}{2}\left(\frac{2m}{\hbar^2}\right)^2\rho\left(\frac{\vec{W}}{f}\right)^2 . \tag{2.41}$$

The spin orbit density only gets contributions from the $\hbar^2$ and higher terms. The lowest-order expression is

$$-\vec{J}_2[\rho] = \left(\frac{2m}{\hbar^2}\right)\frac{1}{f}\rho\vec{W} = \left(\frac{2m^*}{\hbar^2}\right)\rho\vec{W} . \tag{2.42}$$

(A semiclassical spin-orbit correction equivalent to eq. (2.42) for $m = m^*$ has been derived earlier by Stocker et al.[49])

Carrying through the expansion to 4th order with effective mass and spin-orbit is extremely tedious. It has been done with an algebraic computer code by Grammaticos and Voros[30]; we refer to their papers for the explicit expressions for $\tau_4[\rho]$ and $\vec{J}_4[\rho]$. Again, after suitable partial integrations, the relevant contributions to the total energy only contain first and second derivatives of the densities $\rho_q(\vec{r})$. The corresponding expressions are given in ref. 15.

Note that for Skyrme forces $f(\vec{r}) = 1 + \beta\rho(\vec{r})$, and $\vec{W}(\vec{r})$ is proportional to $\vec{\nabla}\rho(\vec{r})$, so that the functionals $\tau[\rho]$ and $\vec{J}[\rho]$ ultimately only contain the density ρ and its gradients. We also recall to the reader that the equations in this section hold for either proton or neutron densities and not for the total densities $\tau = \tau_n + \tau_p$, $\rho = \rho_n + \rho_p$ and $\vec{J} = \vec{J}_n + \vec{J}_p$.

2.5 Summary

Let us summarize at this point the main steps of the derivation and justification of the semiclassical variational method.

1) HF calculations with effective Skyrme interactions allow to calculate a vast amount of nuclear ground-state properties, deformation energies and (with RPA) giant resonances to a satisfactory degree.
2) The HF energy can be split, by means of the Strutinsky averaging procedure, in a selfconsistent average part $\tilde{E}_{HF}$ and a shell-correction part, see eq. (2.14).
3) The averaged energy $\tilde{E}_{HF}$ and the corresponding selfconsistent average densities $\tilde{\rho}_q(\vec{r})$ can be obtained in a strictly variational way.[23] Therefore, by virtue of the Hohenberg-Kohn theorem, $\tilde{E}_{HF}$ and thus $\tilde{\tau}_q(\vec{r})$ and $\vec{\tilde{J}}(\vec{r})$ are unique functionals of $\tilde{\rho}_q(\vec{r})$.
4) The Strutinsky averaging method is practically equivalent to a semiclassical $\hbar$-expansion of the energy,[27] which in turn leads to the ETF density functionals $\tau[\rho]$ and $\vec{J}[\rho]$.
5) The ETF functional $\tau[\rho]$ with gradient corrections up to fourth order reproduces with high accuracy the average kinetic energy of nucleons in realistic potentials.[29,31]
6) Combining 3) and 4) allows to express $\tilde{E}_{HF}$ in terms of $\tilde{\rho}_q(\vec{r})$ only by means of the ETF-functionals $\tau[\rho]$ and $\vec{J}[\rho]$ and to perform semiclassical density variational calculations in order to optimize $\tilde{\rho}_q(\vec{r})$.
7) After selfconsistency has been reached for $\tilde{E}_{HF}$ and $\tilde{\rho}_q(\vec{r})$, the average mean fields eqs. (2.9) - (2.11) can be used to calculate the shell-correction energies $\delta_1 E_q$ (2.16) by solving once the Schrödinger equation (2.17). Adding $\delta_1 E_q$ to $\tilde{E}_{HF}$, thus incorporating the shell effects perturbatively, allows to recover the (exact) HF energy with sufficient accuracy.[15,23]
8) In the case of purely local potentials, the contribution to the total kinetic energy coming from the 4th order correction term $\tau_4[\rho]$ may be simulated by multiplying the Weizsäcker term in $\tau_2[\rho]$ by a factor $\eta \approx 1.4 - 1.5$. However, this procedure does not work for nonlocal Skyrme potentials (where η depends on the effective mass m^*_∞); it also leads to unphysical variational densities, as discussed in sect. 3.1 below.

3. SEMICLASSICAL VARIATIONAL CALCULATIONS

Inserting the functionals $\tau_{ETF}[\rho]$ and $\vec{J}_{ETF}[\rho]$ in the Skyrme energy density eq. (2.2) and making use of the variational definitions of $f_q = m/m_q^*$ and $\vec{w}_q$ by eqs. (2.10), (2.11), we can now express the total average energy of the nucleus as a functional of the spatial densities ρ_q only. The idea then is, as discussed in the introduction, to perform a variational calculation on the densities ρ_q, including Lagrange multipliers λ_q to ensure the correct particle numbers (N and Z):

$$\delta \int d^3r \left\{ \mathcal{E}[\rho_n, \rho_p] - \lambda_n \rho_n(\vec{r}) - \lambda_p \rho_p(\vec{r}) \right\} = 0 \quad . \tag{3.1}$$

(Here $\mathcal{E}[\rho_n,\rho_p]$ contains both the nuclear and the Coulomb parts.) In the following we shall discuss what happens if the variation is done exactly, i.e. if the corresponding Euler-Lagrange equations are solved.

3.1. Discussion of the ETF-Euler Variational Equations

In order to simplify the presentation, we shall again assume only one kind of particles - realistically, one will obtain two coupled differential equations for ρ_n and ρ_p - and leave out the effective mass and spin-orbit contributions (i.e. put $f = 1$ and $\vec{w} = 0$). These restrictions do not affect the conclusions drawn below.

The Euler-Lagrange equation then becomes

$$\frac{\hbar^2}{2m} \left\{ \frac{5}{3} \kappa \rho^{2/3} + D_2[\rho] + D_4[\rho] \right\} + V[\rho] = \lambda \quad , \tag{3.2}$$

where the term in curly brackets comes from the variation of the kinetic energy and the potential is

$$V[\rho] = \frac{\delta \mathcal{E}_{pot}}{\delta \rho} \quad , \tag{3.3}$$

cf. eq. (2.9). The second-order kinetic term is

$$D_2[\rho] = \frac{1}{36} \left[\frac{(\vec{\nabla}\rho)^2}{\rho^2} - 2 \frac{\Delta \rho}{\rho} \right] = \frac{\delta \tau_2[\rho]}{\delta \rho} \quad . \tag{3.4}$$

The term $D_4[\rho]$ correspondingly contains 7 contributions with up to 4th order derivatives of ρ.[29,31] The equation (3.4) can in principle only be solved numerically. However, it is possible to determine rather easily the asymptotic behavior of the solution both inside the nucleus and in the outer surface.

3.1 a) Asymptotic behavior in the outer surface

The fall-off of the density $\rho(r)$ at large distance r (we shall for simplicity assume spherical symmetry) is completely determined by the gradient corrections in the kinetic energy functional $\tau[\rho]$, if they are included at all. We shall accordingly discuss it in three steps.

1- Using $\tau_{TF}[\rho]$ only: If only $\tau_{TF}[\rho]$ is used, eq. (3.2) reduces to

$$\frac{\hbar^2}{2m} \cdot \frac{5}{3} \kappa \rho^{2/3} + V[\rho] = \lambda \quad . \tag{3.5}$$

If the potential $V[\rho]$ contains only powers of ρ and no gradients, the only solution of eq. (3.5) is $\rho(\vec{r}) = \rho_0$ and one obtains thus a liquid drop model type constant density with a sharp cut-off at the surface.

For Skyrme-like forces with a term $b(\vec{\nabla}\rho)^2$ in the potential energy, eq. (3.5) leads to a density profile which near the surface goes like[3]

$$\rho(r) \propto \quad \mathrm{Tgh}^2\left(\frac{r-R_0}{\alpha}\right) \tag{3.6}$$

for spherical nuclei, where α is essentially determined by the constant b in front of the $(\vec{\nabla}\rho)^2$ term. This density thus has to be cut off at a finite radius $r = R_0$ and put equal to zero outside, and is therefore not very physical. It leads to the deficiencies of the calculations reported in ref. 7 which we have already mentioned in the introduction.

2- Using $\tau_{TF}[\rho] + \tau_2[\rho]$: Berg and Wilets[4] pointed out that the inclusion of a Weizsäcker term in the variational equation eq. (3.2) (with $D_4 = 0$) leads to an asymptotic fall-off of the density with the correct exponential form (in the spherical case):

$$\rho(r) \xrightarrow[r\to\infty]{} \frac{1}{r^2} e^{-r/a} \tag{3.7}$$

The range a is given by the Fermi energy λ (which is always negative) and the coefficient of the Weizsäcker term:

$$a = \sqrt{-\frac{1}{36}\frac{\hbar^2}{2m}\cdot\frac{1}{\lambda}} \quad . \tag{3.8}$$

Unfortunately, this range is too small by a factor $\sim$ 2-3 compared with realistic nuclear surfaces. Consequently, the variational densities fall off too quickly in the outer surface and lead to an overestimation of the kinetic energy (which is partially compensated by an overestimation of the potential energy). This was confirmed in numerical calculations by Bohigas et al.,[50] who solved the Euler equations using the local functional $\tau_{TF}[\rho] + \tau_2[\rho]$ eqs. (2.31), (2.32) for a Skyrme force with $m^*_\infty/m \simeq 0.95$ and without spin-orbit force. The semiclassical energies obtained in this way differed from the exact HF energies by $\sim$ 0.4 - 0.6 MeV per nucleon, thus by far more than the order of magnitude of the shell corrections.

To overcome this defect - still in an attempt to solve the relatively easy second order differential equation - several authors used functionals of the type

$$\tau[\rho] = \alpha\rho^{5/3} + \eta\cdot\frac{1}{36}\frac{(\vec{\nabla}\rho)^2}{\rho} + \frac{1}{3}\Delta\rho \quad , \tag{3.9}$$

where α and η were adjustable parameters.[4,46-48,51] In particular in the so-called MTF-functional,[46] η was chosen to be $\sim$ 4-5, in order to obtain realistic tails of the densities, see eq. (3.8). This leads, however, to a drastic overestimation of the kinetic energy - in particular its surface contributions - which was compensated in ref. 46 by reducing the coefficient of the TF term (i.e. $\alpha < \kappa$). In this way it was possible to fit the kinetic energies of spherical nuclei quite well (see also ref. 47). However, the price to be paid for this is that α and β depend on the nucleon number and on the force (in particular on m^*_∞). The latter is obvious since the explicit effective mass and spin-orbit contributions in $\tau_2[\rho]$, shown in eq. (2.41), are ignored in eq. (3.9). Moreover, the MTF-functional[46] completely fails to give reasonable deformation energies due to a drastic overestimation of the surface energy contributions (see the next section).

Treiner and Krivine[48] recently used another functional of the type of eq. (3.9) with the original coefficient of the TF term (i.e. $\alpha = \kappa$) and $\eta = 2$, and added the correct second-order spin-orbit terms (see eqs. (2.41), (2.42)). This functional still slightly overestimates the surface energy, leading to a too high fission barrier as compared to the one obtained with the full, unchanged functional $\tau_{ETF}[\rho]$ including the 4th order contributions (see sect. 3.2). In fact, we have seen in fig. 2 above that a factor of $\eta \simeq 1.4$ to 1.5 would lead to reasonable deformation energies if

spin-orbit and eff. mass contributions are neglected. However, the tails of the density distributions then become unrealistically steep, as seen from eq. (3.8).

One faces thus a basic dilemma when using adjustable functionals of the type of eq. (3.9): If one wants to obtain densities with good tails, one needs $\eta \simeq 4\text{-}5$; if one wants to obtain good energies, and in particular deformation energies, one needs $\eta \simeq 1.4 - 1.5$. (A similar dilemma exists also in atomic physics in the so-called Thomas-Fermi Weizsäcker theory.[52]) We shall see in the next section that this dilemma can be satisfactorily resolved by using the full, unchanged functional $\tau_{ETF}[\rho]$.

3- Using $\tau_{ETF}[\rho]$ up to 4th order: The full fourth order equation (3.2) was discussed in ref. 31. In this case the spherical solution of $\rho(r)$ falls off like

$$\rho(r) \xrightarrow[r\to\infty]{} \frac{c}{r^6} \quad ; \tag{3.10}$$

the coefficient c is given by

$$c = \left[-\frac{\hbar^2}{2m}(3\pi^2)^{-2/3} \cdot \frac{13}{45} \cdot \frac{1}{\lambda}\right]^{3/2} \quad . \tag{3.11}$$

This result at first looks rather discouraging, since eq. (3.10) is not the behavior we would like to expect from a nice density. However, we do not know at which distance from the nuclear surface the behavior r^{-6} will be assumed. In order to investigate this, let us take $\lambda \simeq -7$ MeV. We then find from eq. (3.11) that $c \simeq 0.03$ fm^3. If eq. (3.10) were to be true at a distance of $r = 10$ fm in ^{208}Pb, the density then would be 3×10^{-8} fm^{-3} at that point which is 4 orders of magnitude smaller than what it would be for a Fermi function type density. This indicates that eq. (3.10) is a purely mathematical result which is reached so far outside the nuclear surface that it will have no physical meaning. This is illustrated also in the semi-infinite nuclear matter calculations presented in ref. 15.

Unfortunately, the highly non-linear, fourth order differential equation (3.2) seems unaccessible to numerical solutions. Even in the semi-infinite case, where it can be integrated once analytically, we did not succeed in solving numerically the resulting third order equation. However, the results obtained with a restricted variational space for the densities $\rho_q(\vec{r})$ presented below are satisfactory enough, so that it is not necessary to solve eq. (3.2) exactly.

3.1.b) Asymptotic behavior inside the nucleus

The onset of the surface region, i.e. the deviation of the density from a constant value in the interior of a heavy nucleus, can also be estimated qualitatively without exactly solving the Euler equation. For simplicity we shall ignore the Coulomb interaction and the curvature effects, i.e. take the limit of a very large nucleus. Since in the inner region the density is very near its saturation value, we shall - following Skyrme,[3] and Strutinsky and Tyapin[53] who developed in this way a precursor of the droplet model - replace the Skyrme energy density by a schematic one which, however, preserves the correct saturation properties.

We thus write

$$\mathcal{E}[\rho] = \rho\tilde{e}_\infty(\rho) + a(\vec{\nabla}\rho)^2 + \frac{\hbar^2}{2m}(\tau_2[\rho]+\tau_4[\rho]) \qquad (3.12)$$

where the "volume part" $\tilde{e}_\infty(\rho)$ is taken to be

$$\tilde{e}_\infty(\rho) = a_v^\infty + \frac{K_\infty}{18\rho_\infty^2}(\rho-\rho_\infty)^2 \quad . \qquad (3.13)$$

This corresponds to a parabolic approximation of the saturation curve near the saturation density ρ_∞, which certainly is good enough for the following estimations. Writing

$$\rho(r) = \rho_\infty y(r) \, , \qquad (3.14)$$

the Euler equation then becomes (neglecting the curvature contribution)

$$\frac{K_\infty}{18}(3y^2-4y+1) - 2a\rho_\infty y'' + \frac{\hbar^2}{2m}(D_2[y]+D_4[y]) = 0 \, , \qquad (3.15)$$

where $y'' = d^2y/dr^2$. The kinetic terms D_2 and D_4 play a minor role in the following development and we shall therefore drop $D_4[\rho]$ immediately. To arrive at eq. (3.15) we have also neglected the fact that the central density in finite nuclei is in general different from the saturation density ρ_∞ [54]; this has little bearing on the following argument and shall shortly be discussed in sect. 3.3.

We now write

$$y(r) = 1 - e^{(r-R)/\alpha} = 1 - \varepsilon(r) \quad . \qquad (3.16)$$

Inside the nucleus, $\varepsilon(r) \ll 1$ and we can expand eq. (3.15) in powers of ε. Keeping the linear terms in ε, we obtain an equation for α:

$$\alpha = \sqrt{\frac{18}{K_\infty}\left(a\rho_\infty + \frac{1}{36}\frac{\hbar^2}{2m}\right)} \quad . \tag{3.17}$$

For realistic Skyrme forces, $b\rho_\infty \simeq$ (10 - 13) MeV fm^2, so that α turns out to be of the order of $\sim$ 1 fm. The Weizsäcker correction (the second term in the brackets in eq. (3.17)) only contributes $\sim$ 3 % to this result; the term $D_4[\rho]$ in eq. (3.15) would have contributed even far less.

We learn from this that the asymptotic inner part of the nuclear surface is mainly determined by the "surface term" $a(\vec{\nabla}\rho)^2$ of the Skyrme energy density and by the incompressibility K_∞; the kinetic energy gradient terms play only a minor role here. The range α of the inner surface part is $\sim$ 1 fm and thus about twice larger than the typical value of the diffuseness parameter of the density when parametrized by a Fermi function. This tends to make the realistic densities asymmetric around the half-density distance; the "shoulder" of the surface is broader than the tail of the surface. This asymmetry is, indeed, seen in the results discussed in sect. 3.2 below.

In order to summarize this section, let us repeat the main conclusions we have reached.

1- If the functional $\tau_{ETF}[\rho]$ is used to solve the Euler-Lagrange variational equation for the density, the gradient corrections to $\tau_{ETF}[\rho]$ completely determine the asymptotic fall-off of the density in the extreme surface. In no order of its gradient expansion can $\tau_{ETF}[\rho]$ give a realistic exponential fall-off. In particular with the gradient terms kept up to 4th order, one obtains a fall-off of the form $1/r^6$.

2- This latter result need not be in contradiction with the positive numerical results quoted in sect. 2.4 in the sense that the mathematical fall-off $\sim 1/r^6$ is only assumed at far distances outside the nucleus which play no physical role, whereas a realistic surface region is compatible with the 4th order functional $\tau_{ETF}[\rho]$.

3- Heuristic functionals $\tau[\rho]$ with only second order corrections and adjustable coefficients can either reproduce energies or density profiles, but not both at the same time.

4- Practically independently of the gradient corrections to $\tau[\rho]$, the inner asymptotic part of the surface is essentially determined by a balance between the gradient term $\sim(\nabla\rho)^2$ of the potential energy and the incompressibility K_∞. As a consequence, the density profile is in general asymmetric around its inflection point.

3.2 Variational Calculations for Finite Nuclei

In the following we shall present some selective results of variational semiclassical calculations[15] obtained with a restricted, but flexible variational space of trial nuclear densities. We shall

be brief and refer the interested reader to the review article[15] in which these calculations have been discussed in detail.

For spherical nuclei we chose the radial densities to have the form (see also ref. 55):

$$\rho_q(r) = \frac{\rho_{0q}\left[1 + \rho_{1q}\exp\left(-r^2/\beta_q^2 R_q^2\right)\right]}{\left[1+\exp\left(\frac{r-R_q}{\alpha_q}\right)\right]^{\gamma_q}} \quad . \qquad (q = p,n) \qquad (3.18)$$

We have thus 10 independent variational parameters ρ_{0q}, ρ_{1q}, β_q, α_q, and γ_q, with respect to which the total energy is minimized; the radius constants R_q are always determined to fix the nucleon numbers Z and N. For $\rho_{1q} = 0$ and $\gamma_q = 1$ we have the familiar Fermi functions with central density ρ_{0q} and surface diffuseness α_q. For $\gamma_{1q} \neq 1$, the surface is asymmetric; as we have discussed in sect. 3.1, we expect $\gamma_q > 1$ in realistic cases. For $\rho_{1q} \neq 0$, the Gaussian factor in eq. (3.18) allows for a depression or an enhancement in the central region measured by β_q; for physical reasons we are interested only in values $0.3 \lesssim \beta_q < 1.0$. (In fact, the energy was found to be stationary for $\beta_q \simeq 0.5$ in all cases where $\rho_{1q} \neq 0$ was favored at all.[15,55])

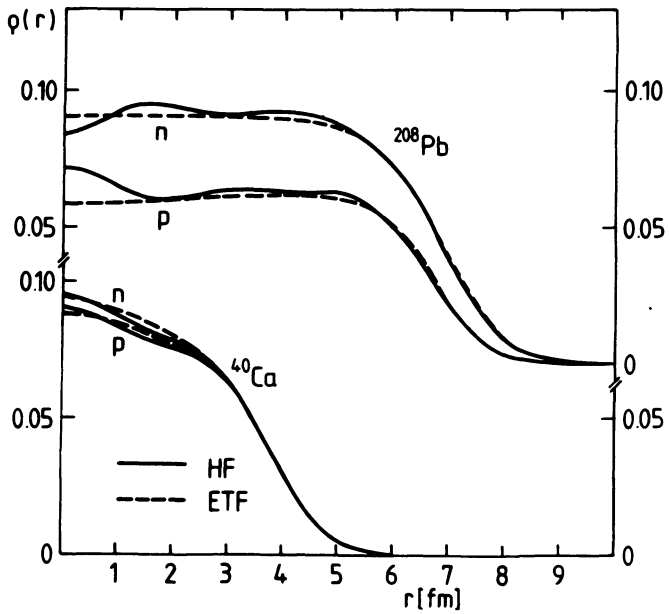

Fig. 3. Comparison of the microscopical HF densities and the variational ETF densities for ^{40}Ca and ^{208}Pb, obtained with the Skyrme force SkM*.

In figure 3 we compare the density profiles obtained for ^{40}Ca and ^{208}Pb with microscopical HF results, both calculated with the Skyrme force SkM*.[15,16] An almost perfect agreement is obtained in the surface and the tail region. In the interior part the ETF densities reproduce nicely the average trend of the HF results. In fact the possibility to build up a bump or a dip near the center, although it does not affect the binding energies by more than a few hundred keV, is important for obtaining this agreement. In particular for ^{40}Ca, we see that the central densities are enhanced by $\sim$ 20 %. It is worth underlining that this is not just a shell effect, but it must be understood as a bulk effect which results from the compression of the nucleus by the surface tension. In heavy nuclei such as ^{208}Pb, this compression effect is overpowered by the Coulomb repulsion between the protons, which leads to a slight depression at the center ($\sim$ 8 % for the proton and $\sim$ 2 % for the neutron density of ^{208}Pb).

In table 1 we present the binding energies of a series of spherical nuclei (all in MeV). B_{exp} are the experimental values; B_{HF} and B_{ETF} the HF and the ETF results (with SkM*). (In both calculations, a 1-body c.m. energy correction [16] has been included; it is not included in all the other results presented below.) Note the nice agreement between B_{HF} and B_{exp} especially for the ß-stable nuclei. The semiclassical energies B_{ETF}, which of course do not contain

Table 1

	B_{exp}	B_{HF}	B_{ETF}	B_{EVM}
^{16}O	127.6	127.7	128.0	127.4
^{40}Ca	342.1	341.1	345.9	340.4
^{48}Ca	416.0	420.1	421.8	418.4
^{56}Ni	484.0	485.4	483.9	483.1
^{90}Zr	783.9	784.5	786.6	782.7
^{114}Sn	971.6	969.2	976.0	967.9
^{132}Sn	1102.7	1110.7	1101.5	1108.3
^{140}Ce	1172.7	1173.9	1174.5	1171.6
^{208}Pb	1636.5	1636.4	1627.0	1633.7

the shell effects, are larger than the averaged HF energies by $\sim$ 3-8 MeV. This effect of a slight overbinding was observed earlier with other Skyrme forces[14] - it is larger by a factor of roughly 2 for the SIII force,[35] presumably due to its larger incompressibility - and must be considered as a slight defect of the ETF functionals. Although the variational principle holds strictly for the "ideal" (but unknown) exact functional $\mathcal{E}[\rho]$, the use of approximate functionals can lead to violations of the variational principle and thus to such overbinding effects. This slight deficiency of B_{ETF} is, however, healed after inclusion of the shell effects by the "expectation value method" (EVM),[56,57] which corresponds to performing a single HF iteration using the variational ETF densities as an input. The so obtained energies are shown in the last column of table 1 and are seen to reproduce the HF energies to within less than $\sim$ 1 MeV (^{16}O, ^{40}Ca) to $\sim$ 3 MeV (^{208}Pb).

In refs. 15,16 it was shown that also the HF neutron and proton r.m.s. radii - and in particular their difference, the so-called "neutron skin" - are also very accurately reproduced by the variational ETF calculations (the shell effects are practically negligible here).

This excellent agreement between the ETF and the (averaged) HF results for both energies and densities demonstrates the powerfulness of the 4th-order corrected ETF functionals; it cannot be obtained leaving out the $\tau_4[\rho]$ term, as discussed above.

In figure 4 we compare the variational ETF charge densities of 5 spherical nuclei to the experimental ones deduced from electron scattering experiments. A very good agreement is found for the average trends in all cases; the remaining differences are the typical shell fluctuations. (These are overestimated in HF calculations with most effective forces; see, however ref. 37 for a recent discussion of this effect.)

As already indicated above, the deviations of constant densities in the nuclear interior - governed by the parameters ρ_{1q} and β_q in eq. (3.18) - have very little influence on the total energy of the nucleus. This is demonstrated in table 2, where we list all the density parameters according to eq. (3.18) together with the minimized energies E_{ETF} of the 5 nuclei shown also in fig. 4. For ^{40}Ca and ^{208}Pb we also give the results obtained when the densities were restricted to pure Fermi functions (imposing $\gamma_q = 1$, $\rho_{1q} = 0$) or asymmetric Fermi functions (with $\gamma_q \neq 1$, but $\rho_{1q} = 0$). It is interesting to note that the 10 parameter variation lowers the total energy by only 2.3 MeV in ^{40}Ca (i.e. $\sim$ 0.7 %) and by 5.1 MeV in ^{208}Pb (i.e. $\sim$ 0.03 %) compared to the 4 parameter variation with pure Fermi functions. Furthermore, almost all of this gain in energy is already obtained with flat densities ($\rho_{1q} = 0$) with an asymmetric surface ($\gamma_q \neq 1$). As long as one is interested in binding or deformation energies alone, it is thus

Table 2

	ρ_{op}	ρ_{on}	α_p	α_n	γ_p	γ_n	ρ_{1p}	ρ_{1n}	$\beta_n=\beta_p$	R_p	R_n	E_{ETF}
^{40}Ca	0.0776	0.0804	0.472	0.464	1.0	1.0	0.0	0.0	-	3.761	3.720	-327.46
	0.0804	0.0834	0.577	0.580	1.43	1.49	0.0	0.0	-	3.999	3.984	-329.35
	0.0768	0.0777	0.566	0.553	1.42	1.42	0.136	0.199	0.5	4.027	4.001	-329.71
^{208}Pb	0.0610	0.0887	0.440	0.530	1.0	1.0	0.0	0.0	-	6.753	6.839	-1604.0
	0.0622	0.0911	0.532	0.662	1.42	1.47	0.0	0.0	-	6.981	7.202	-1608.9
	0.0639	0.0904	0.557	0.646	1.45	1.50	-0.086	-0.004	0.5	6.976	7.125	-1609.1
^{58}Ni	0.0756	0.0800	0.561	0.557	1.42	1.45	0.107	0.168	0.5	4.550	4.552	-491.6
^{116}Sn	0.0697	0.0870	0.559	0.605	1.48	1.50	0.019	0.078	0.5	5.734	5.854	-976.6
^{124}Sn	0.0664	0.0902	0.551	0.630	1.48	1.50	0.017	0.061	0.5	5.828	2.995	-1037.1

Parameters of the variational ETF densities for $\frac{5}{-3}$ spherical nuclei (obtained with SkM*). ρ_{0q} in fm^{-3}, α_q and R_q in fm. The last column shows the total energy in MeV. The underlined values have been imposed in the variational calculations.

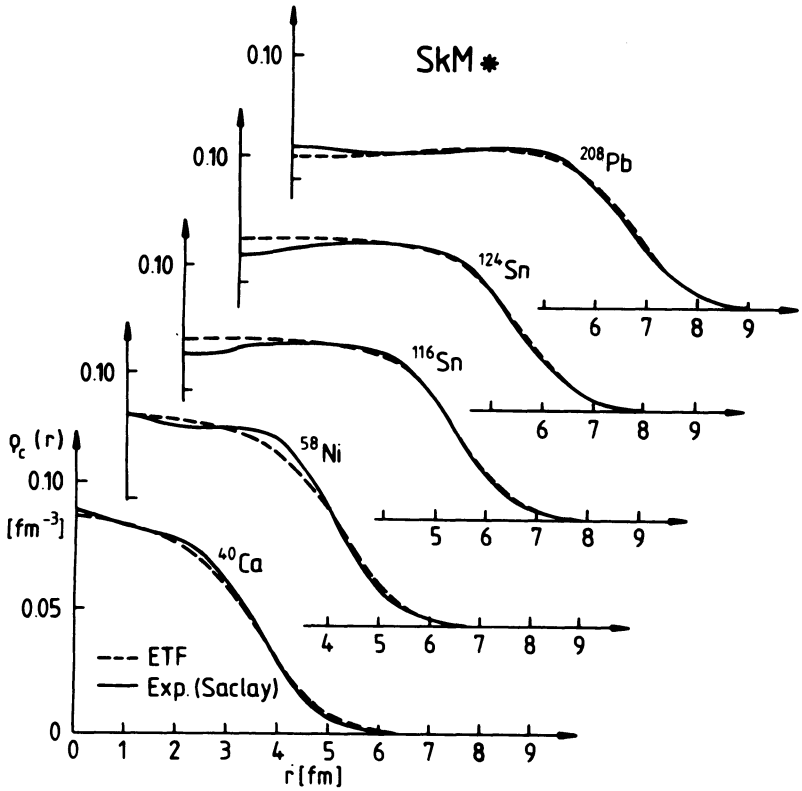

Fig. 4. Comparison of semiclassical ETF charge densities (including a proton form factor of 0.64 fm^2) with the experimental distributions extracted from electron scattering data [58] for five spherical nuclei.

perfectly sufficient to use 3-parameter densities (i.e. Fermi functions to the power γ_q) with a flat interior. The values of γ_q vary only a little, from $\sim$ 1.4 in light to $\sim$ 1.5 in heavy nuclei. For forces with larger K_∞ , the γ_q become smaller, as can easily be understood on the basis of the discussion in sect. 3.1 above. (For the SIII force, e.g., $\gamma_q \sim 1.2$.) When the $\tau_4[\rho]$ gradient corrections are omitted,[48,55] unphysically large values $\gamma_q \sim$ 2-3 are obtained.

In order to describe deformed nuclei, we have to use a constraint since in a semiclassical model all nuclei are spherical in their ground states. In ref. 15 the constraint was introduced by starting from a deformed LDM "generating surface" with sharp edges, such as it has been used in shell-correction calculations for fission

barriers.[22] It was then assumed that the diffuse densities have a constant surface thickness, so that they can be described simply by replacing $(r-R_q)$ in eq. (3.18) by the normal distance from the generating LDM surface (see the details in ref. 15); hereby the density profiles of eq. (3.18) were, for the reasons just given above, restricted to asymmetric Fermi functions ($\gamma_q \neq 1$ but $\rho_{1q} = 0$).

In figure 5 we present the semiclassical fission barriers of ^{204}Pu obtained for four different Skyrme forces. The (c,h) family of shapes[22] was used for which c is the main elongation parameter and h is a "necking" parameter. The cross indicates the location of the empirical LDM saddle point as it is known from shell-correction calculations.[22] We see that the forces SIII[35] and Ska[59] give too high fission barriers by a factor of $\sim$ 2. For the SIII force, this had been known from constrained HF calculations.[60]

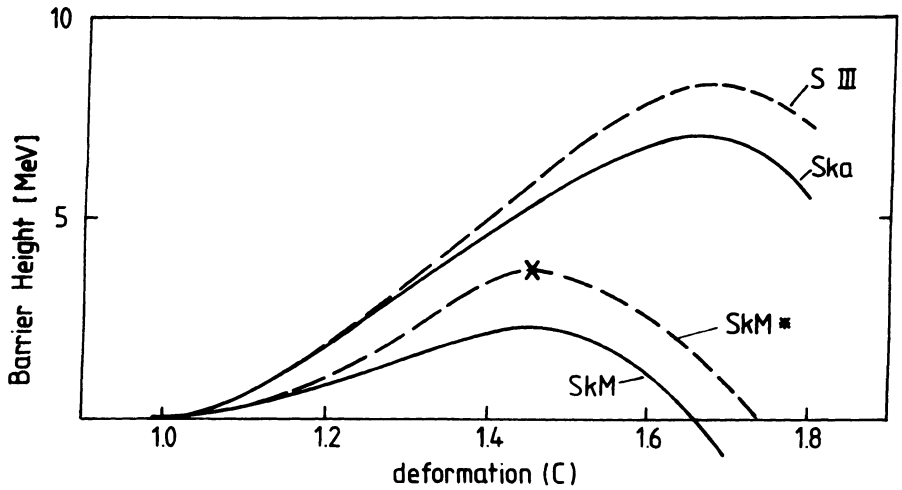

Fig. 5. Semiclassical fission barriers for ^{204}Pu. For each elongation c, the energies are minimized with respect to the neck parameter h. Four different Skyrme forces were used; the cross indicates the empirical LDM saddle point.

In fact, it was a puzzle for quite some time that HF calculations consistently led to too high fission barriers even with effective forces[60,61] which otherwise gave good results for ground state properties of both spherical and deformed nuclei (see a review article[62] on the status of fission barrier calculations up to 1979). Due to the excessive computer times required by the constrained HF calculations for heavy nuclei, it was practically not possible to refit the forces taking explicitly the fission barriers into account. This became, however, possible[63,14,15] with the semiclassical method described

above which is more than 10^3 times faster if one is not interested in the shell effects. As we see from fig. 5, we can well distinguish the average barriers predicted with the different forces.

The Skyrme force SkM which was fitted to reproduce the giant nuclear monopole and quadrupole resonances[51] and therefore has an incompressibility K_∞ of 216 MeV, compatible with eq. (2.12), gives a somewhat too low barrier. (The forces SIII and Ska have higher values of K_∞; which leads to stiffer surfaces and thus to higher surface energies.) The force SkM* was explicitly adjusted with semiclassical calculations to reproduce the LDM saddle point energy[15]; it was shown at the same time to yield excellent binding energies and radii for stable spherical nuclei in HF calculations[16] (see the results shown in figs. 3,4 and table 1 above).

In fig. 6 we present a microscopical test of the semiclassical results. The corresponding HF calculations were done in ref.[16] The figure shows the full HF result, obtained with the SkM force, with

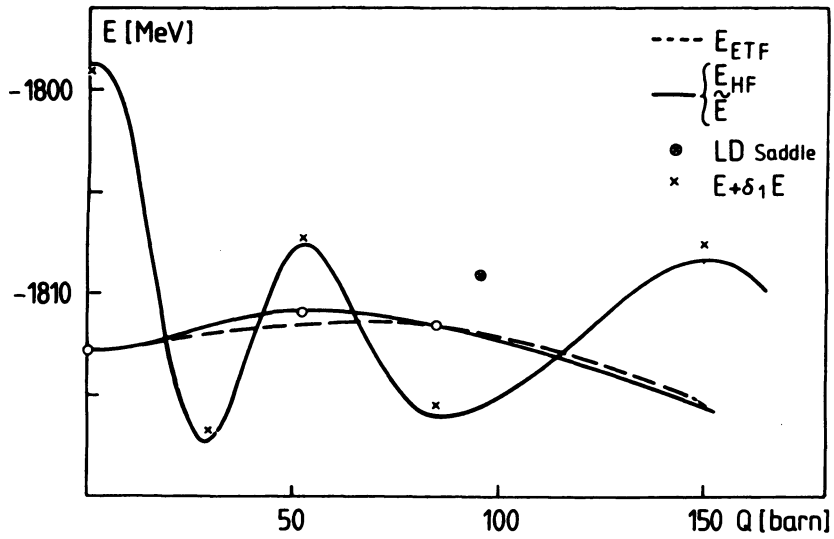

Fig. 6. Fission barrier of ^{204}Pu, calculated with the SkM force. The exact and Strutinsky-averaged HF results[16] are shown along with the semiclassical ETF result.[15] Q is the total quadrupole moment. The cross in a circle indicates the LDM saddle point. The crosses show the results after inclusion of the shell-correction energy $\delta_1 E$.

2 minima and 2 maxima. Also shown is the selfconsistently Strutinsky smoothed HF energy, calculated as discussed in sect. 2.3. The semiclassical ETF result is shown by the dashed line (adjusted at Q = 0).

The agreement of the two average curves is better than 1 MeV at all deformations included. This gives once again a nice confirmation of the semiclassical method. It shows in particular also that the slight overbinding of the ETF results discussed above ($\sim$ 8 MeV in this nucleus) does not affect the deformation energies noticably. The crosses in fig. 6 show the results obtained after adding the shell-correction energy $\delta_1 E$ to the average curves; they reproduce the exact HF values within less than 0.5 MeV.

An interesting result is that in the semiclassical variational calculations, the density parameters ρ_{oq}, α_q, γ_q and R_q found for the spherical shape vary only very little with deformation; in fact, only an error of $\sim$ 0.5 MeV would be made for the realistic force SkM* if they were kept constant.[15] The influence of the asymmetry of the surface, governed by the parameters γ_q, on the fission barrier is shown in fig. 7, where the barrier of ^{204}Pu has been calculated once with $\gamma_q = 1$ and once with the variational values $\gamma_q \neq 1$. The difference is seen to be $\sim$ - 0.8 MeV at the saddle, corresponding to a decrease

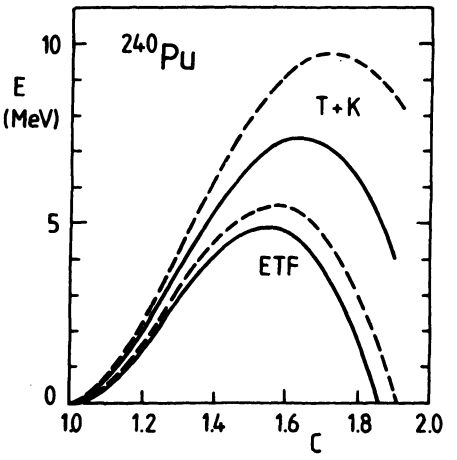

Fig. 7. The same as fig. 5 with force SkM*. The curves ETF show results obtained with the full 4th order functional $\tau[\rho]$ the curves "T + K" those with the phenomenological functional of Treiner and Krivine.[48] Dashed curves are obtained with Fermi function densities ($\gamma_q = 1$), solid curves with asymmetric density profiles ($\gamma_q \neq 1$).

of $\sim$ 0.3 MeV of the surface energy (see sect. 3.3). This difference is typical for forces which give approximately correct average fission barrieres.

We also show in fig. 7 the results obtained for the same force SkM*, but with the simplified functional $\tau[\rho]$ of Treiner and Krivine[48] where τ_4 was omitted and the Weizsäcker coefficient was multiplied by two. It leads to an overestimation of the barrier height.

The corresponding variational values of γ_q were found to be $\gamma_p \simeq 3.2$ and $\gamma_u \simeq 2.3$, reflecting a too steep tail of the densities. A similar calculation with the MTF functional[46] (in which the Weizsäcker term is multiplied by $\sim$4) gives a fission barrier of over 30 MeV for ^{204}Pu. This illustrates the problem discussed above in sect. 3.1 with readjusted functionals $\tau[\rho]$ without 4th order gradient terms.

3.3 Calculation of LDM parameters for Effective Forces

An interesting application of the variational ETF calculations with parametrized densities is the determination of the LDM parameters for a given effective force. Nuclei with $A \gtrsim 40$ are "leptodermous",[54,63] i.e. the ratio of the surface diffuseness α to the bulk radius R is small:

$$\alpha/R \ll 1 \quad . \tag{3.19}$$

The expansion of the nuclear binding energy in powers of α/R is the underlying technique of the liquid drop model.[63] If asymmetry and compression effects are taken into account by further expansions in powers of the small parameters δ and ε, defined by

$$\delta = \frac{\rho_{0n} - \rho_{0p}}{\rho_0} \quad , \qquad (\rho_0 = \rho_{0n} + \rho_{0p}) \tag{3.20}$$

$$\varepsilon = -\frac{1}{3}\frac{(\rho_0 - \rho_\infty)}{\rho_\infty} \quad , \tag{3.21}$$

one obtains the droplet model.[53,54]

The "leptodermous expansion" in powers of α/R was recently adapted to the total energy of an arbitrarily deformed nucleus within the Skyrme-ETF fomalism.[15,64] We refer to the recent review article[15] for the details and quote here just some of the main results. (For earlier calculations of surface energies from ETF results see ref. 30; similar analyses based on semiclassical[48,55] and HF calculations[65-67] may also be compared.)

For symmetric nuclei (N=Z; δ=0) the expansion in powers of α/R leads to

$$E = a_v A + a_s A^{2/3} + a_c A^{1/3} + a_0 + \ldots \qquad (3.22)$$

The dependence of the a_n on the deformation and the force parameters can be exactly separated. For their spherical part, one then expands

$$a_v = a_v^\infty + \frac{1}{2} K_\infty \varepsilon^2 + \ldots \qquad (3.23)$$

$$a_s = a_s^\infty - 3\dot{a}_s \varepsilon + \frac{9}{2} \ddot{a}_s \varepsilon^2 + \ldots \qquad (3.24)$$

$$a_c = a_c^\infty - 3\dot{a}_c \varepsilon + \frac{9}{2} \ddot{a}_c \varepsilon^2 + \ldots \qquad (3.25)$$

etc. Minimizing the energy with respect to ε (fixing the surface parameters α and γ of the densities, which vary only very little for finite nuclei), one obtains the smooth variation of ε with A which reflects the effect of compression of the nucleus by the surface tension:

$$\varepsilon(A) = \frac{3\dot{a}_s A^{-1/3} + 3\dot{a}_c A^{-2/3}}{K_\infty + 9\ddot{a}_s A^{-1/3} + 9\ddot{a}_c A^{-2/3}} \quad . \qquad (3.26)$$

It was shown[15] that for the realistic force SkM*, eq. (3.26) is needed to describe the A-dependence of the central density ρ_0 correctly, whereas the droplet model expression[54]

$$\varepsilon_{DM}(A) = (3\dot{a}_s / K_\infty) A^{-1/3} \quad , \qquad (3.27)$$

which just contains the leading term of eq. (3.26) leads to large overestimations of ε in particular for medium and lighter nuclei. The surface compressibility parameter $\ddot{a}_s$, which is neglected in the droplet model, is known to play an important role for the compressibility of finite nuclei[18,36,68] which nowadays is known from the measurement of the nuclear breathing mode.

In table 3 we list the coefficients of the expansions in eqs. (3.24) and (3.25) (all in MeV), obtained from semi-infinite (symmetric) nuclear matter calculations with the variational ETF method (asymmetric Fermi profiles with $\gamma_q \neq 1$ were used).[15] The various Skyrme forces already mentioned above were used as well as the energy density of Tondeur[69] which is very similar to that of a Skyrme force. Table 3 also contains the effective curvature energy a_c defined by

$$a_c^* = a_c^\infty - \frac{9\dot{a}_s^2}{2K_\infty} \qquad (3.28)$$

which is obtained[54] if the lowest order contribution from ε is included in eq. (3.22).

In the realistic case one has to include also the Coulomb energy and to expand everything also in powers of the asymmetry parameter δ eq. (3.20). We refer to the droplet model of Myers and Swiatecki[54] for this procedure. In table 4 we list the coefficients (in MeV) of the surface energy which are obtained if it is expanded to second order in the asymmetry parameters (for a fixed value of ε)[54]

$$a_s = a_s^\infty + H\tau^2 + 2P\tau\delta - G\delta^2 \quad ; \qquad (3.29)$$

hereby τ is the so-called "neutron skin" parameter:

$$\tau = \frac{R_n - R_p}{r_0} \simeq \frac{2}{3}(I - \delta)A^{1/3} + O(A^{-1/3}) \qquad (3.30)$$

with I = (N-Z)/A. We also give in table 4 the volume asymmetry energy J and the "surface stiffness coefficient" Q of the droplet model, defined by

$$Q = \frac{H}{\left(1 - \frac{2}{3}\frac{P}{J}\right)} \quad , \qquad (3.31)$$

as well as the quantity $\tilde{J}$

$$\tilde{J} = \frac{2}{3}\left(P + \frac{GH}{P}\right) \qquad (3.32)$$

of which a theorem derived by Myers and Swiatecki[54] tells that it should be equal to J. The same 5 effective forces as in table 3 were used; on the top line (quoted "DM") we also give the droplet model values. We see that for all forces, the theorem $\tilde{J} \equiv J$ is fulfilled within less than 3 % which may be considered as a test of the numerical calculations. (To obtain the results in table 4, pure Fermi functions with $\gamma_q = 1$ were used, because the above droplet model relations do not apply to density profiles with asymmetric surfaces.[15])

In summary it can be said that the variational ETF calculations can be used to justify and test the droplet model or similar extensions of the simple LDM. Some of the shortcomings of the droplet model have been discussed and some extensions and improvements have been proposed.[15] The main conclusion is that the variational ETF formalism with its 8 - 10 Skyrme force parameters is more powerful than the droplet model, even if the latter is extended to include some 20 or more phenomenological parameters.

Table 3

Force	a_s^∞	$\dot{a}_s$	$\ddot{a}_s$	a_c^∞	$\dot{a}_c$	$\ddot{a}_c$	a_o^∞	a_c^*
SIII	18.04	-12.40	-88.11	9.52	26.02	49.32	- 8.66	7.57
Ska	18.52	-11.60	-71.29	12.15	30.20	47.28	-13.88	9.86
SkM	16.60	-11.06	-58.64	12.19	27.26	37.27	-12.31	9.65
SkM*	17.22	-11.15	-60.37	12.82	29.27	40.76	-14.13	10.24
Tond.	18.11	-11.30	-65.19	12.74	30.25	44.23	-14.73	10.32

Table 4

force	a_s^∞	H	P	G	J	Q	$\tilde{J}$
DM	18.56	9.42	17.55	45.4	28.06	16.1	27.94
SIII	18.13	13.55	31.76	26.52	28.16	54.6	28.72
Ska	18.79	10.66	31.69	47.47	32.91	29.8	31.77
SkM	16.85	11.11	31.99	38.94	30.75	36.3	30.34
SkM*	17.51	10.56	31.61	39.04	30.03	35.4	29.77
Tondeur	18.41	11.46	33.24	39.83	32.12	37.0	31.32

4. EXTENSIONS OF THE SEMICLASSICAL METHOD

4.1. Partial Resummation of the Wigner-Kirkwood $\hbar$ Expansion

One of the unpleasant features of the $\hbar$-expanded densities $\rho_{ETF}(\vec{r})$ and $\tau_{ETF}(\vec{r})$ eqs. (2.26), (2.27) is their divergence at the classical turning points. It is the reason why they cannot be used directly in an iterative procedure to calculate the selfconsistent average HF potential. One way to circumvent this problem is the construction of the ETF functional $\tau_{ETF}[\rho]$ and its use in a density variational calculation, as we have discussed it extensively above.

Another way to solve the turning point problem is the use of partial resummations of the Wigner-Kirkwood expansion of the Bloch density matrix C eq. (2.25). Bhaduri[70] noticed that all terms which contain powers of the first gradient of the potential, $\vec{\nabla}V(\vec{r})$, can be summed up to infinite order in $\hbar$. In this way one obtains for the local Bloch density

$$C(\vec{r},\vec{r}';\beta) = C_{TF}(\vec{r},\vec{r}';\beta)\, e^{\frac{\hbar^2}{24m}\beta^3(\vec{\nabla}V)^2}\{1+\hbar^2\eta_2+\hbar^4\eta_4+\dots\}\,, \qquad (4.1)$$

where C_{TF} is given by eq. (2.24) and the η_n contain second and higher order gradients of $V(\vec{r})$. The nice feature of eq. (4.1) is that it leads, after Laplace inversion, to densities $\rho(\vec{r})$ and $\tau(\vec{r})$ which are well-behaved everywhere in space, being in particular finite at the classical turning points and falling rapidly to zero in the classically forbidden region. Noting that the exponential factor appearing in eq. (4.1), in fact, is the Laplace transform of the Airy function, we see that in the lowest order in eq. (4.1) (i.e. neglecting η_2, η_4, etc.) one obtains by eq. (2.20) the folding product of the TF density matrix with an Airy function

$$\rho(\vec{r},\vec{r}') = \sigma(\vec{R})\int_{-\infty}^{\lambda}\rho_{TF}(\vec{r},\vec{r}';\lambda-E)\,\mathrm{Ai}[-\sigma(\vec{R})E]\,dE\,, \qquad (4.2)$$

where

$$\sigma(\vec{R}) = \sigma\left(\frac{\vec{r}+\vec{r}'}{2}\right) = \left(\frac{8m}{\hbar^2}\right)^{1/3}\{[\vec{\nabla}V(\vec{R})]^2\}^{-1/3}. \qquad (4.3)$$

It can be shown[71] that this result eq. (4.2) is identical to that of a locally linear approximation to the potential V.

The above procedure can be extended to sum up also all terms containing second order gradients to all powers; this corresponds to a locally harmonic approximation to $V(\vec{r})$.[71] (Nonlocal potentials can be treated in the same way.)

The densities obtained after these partial resummations have some unphysical oscillations in the interior part of the nucleus. They can be damped out if the Laplace inversion eq. (2.20) is not done analytically, but with the saddle point method, hereby using only the saddle point $\beta_0 > 0$ on the real β axis.[70] This implicitly is a semiclassical approximation; as shown by Jennings,[26,43] the average (or ETF) part of the densities $\rho(\vec{r})$, $\tau(\vec{r})$ comes from contributions in the inverse Laplace transform from the region around $\beta = 0$, whereas poles (or saddle points) of $C(r,r';\beta)$ far from the real β axis - they usually ly on or near the imaginary β axis - lead to the fluctuating part (shell effect).

The combined method of partial resummation of $C(r,r';\beta)$ and using the saddle point method (with real $\beta_0 > 0$) for the Laplace inversion leads thus to well-behaved semiclassical densities $\rho(\vec{r})$ and $\tau(\vec{r})$ (see ref. 72 for a discussion of some technical details and model examples). These densities can be used directly to calculate the average HF-Skyrme potentials eqs. (2.9) - (2.11) and thus, in an iterative cycle, to reach selfconsistency.

Compared to the variational ETF method discussed in the main parts of these lectures, the present method has the advantage that one does not need to know the functional $\tau[\rho]$. Numerically, the densities tend to become unstable since hihger and higher gradients of the potential are implicitly taken during the iterative cycle. They therefore have to be regularized e.g. by a fit to smooth parametrized densities.[73] It was found that when the same form of the densities was used as in eq. (3.18) above, the partial resummation method leads to very similar results as the variational ETF method using the functionals $\tau_{ETF}[\rho]$ and $\vec{J}_{ETF}[\rho]$; in particular the LDM and droplet model parameters reported in tables 3,4 above are closely reproduced,[74] thus implicitly providing a quantitative confirmation of the ETF functionals.

4.2. Semiclassical Description of Hot Nuclei and Nuclear Matter

Excited nuclear systems with temperatures larger than $\sim$ 3 MeV contain no shell effects and are therefore ideal objects for semiclassical investigations. Such hot compound nuclei can be produced in heavy ion and high-energy hadron induced reactions.[75] In astrophysics, there has recently been an increased interest in the equation of state of hot nuclear matter.[76,77]

The microscopical mean field (HF) theory can easily be generalized to finite temperatures in the statistical approximation.[78] Here one minimizes no longer the total intrinsic energy E, but the Helmholtz free energy F

$$F = E - TS \ , \tag{4.4}$$

where the entropy is given by

$$S = -\sum_{q\nu} [n_\nu^q \ln n_\nu^q + (1 - n_\nu^q) \ln(1 - n_\nu^q)] \tag{4.5}$$

in terms of the occupation numbers

$$n_\nu^q = \frac{1}{1+\exp\left(\frac{\varepsilon_\nu^q - \lambda_q}{T}\right)} \ . \tag{4.6}$$

(We put the Boltzmann constant $k \equiv 1$ and measure the temperature T in units of MeV.)

HF calculations at finite temperature are relatively easy to perform; it is sufficient to replace the HF occupation numbers n_ν^q in eqs. (2.3) - (2.5) by the occupation numbers eq. (4.6). Such calculations have been performed with Skyrme forces by different groups.[77,79-81] Hereby it must be assumed that the parameters of the Skyrme force themselves do not depend on T. This could in principle be checked by performing a Brückner G-matrix calculation at finite temperature; this has, however, not been endeavoured so far.

A well-known effect of the smoothing of the Fermi surface brought about by the occupation numbers eq. (4.6) is the washing out of the shell effects; the above mentioned HF results showed that beyond a critical temperature $T_c \simeq$ (2.5-3) MeV (which is roughly the same for all systems) the shell effects have disappeared. Systems at such temperatures are thus ideal objects for studies within a semi-classical framework. It is therefore obvious to try to apply the methods developed above to nuclei at $T > 0$. Thomas-Fermi calculations at finite temperature are by now standard.[76,82,83] However, we shall see in the following that it is not easy to construct the appropriate ETF functionals for $T > 0$.

The Wigner-Kirkwood expansion discussed in sect. 2.4 can easily be extended to finite temperatures. To do so, it is sufficient to know that the inclusion of the Fermi occupation numbers eq. (4.6) in the HF case is identical to a convolution of the spectral density with the function $f_T(E) = \frac{1}{4} \ \mathrm{Cosh}^{-2}(E/2T)$.[23] Thus, due to the convolution theorem, the Bloch density eq. (2.19) is multiplied for $T > 0$ with the Laplace transform of $f_T(E)$

$$C_T(\vec{r},\vec{r}';\beta) = C(\vec{r},\vec{r}';\beta) \frac{\pi\beta T}{\sin(\pi\beta T)} \ . \tag{4.7}$$

Note that this result is still exact within the HF framework. Proceeding now as in the $T = 0$ case, i.e. replacing the "cold" Bloch

density C by its Wigner-Kirkwood expansion eq. (2.25) and doing the inverse Laplace transforms term by term, one finds the expressions for the densities $\rho_{ETF}(\vec{r})$ and $\tau_{ETF}(\vec{r})$ at T > 0 and that of the entropy density $\sigma(\vec{r})$ defined by

$$S = \int d^3r\, \sigma(\vec{r}) = -\frac{\partial F}{\partial T} \quad . \tag{4.8}$$

The resulting expressions are up to order $\hbar^2$ (for a local potential, with effective mass m*),[84]

$$\rho^T_{ETF}(\vec{r}) = \frac{1}{2\pi^2}\left(\frac{2m^*}{\hbar^2}\right)^{3/2} \times \{T^{3/2} J_{1/2}(\eta) + \tag{4.9}$$
$$+ \frac{1}{24}\frac{\hbar^2}{2m^*}\left[\frac{3}{4}T^{-3/2} J_{-5/2}(\eta)(\vec{\nabla}V)^2 + T^{-1/2} J_{-3/2}(\eta)\Delta V\right]\} \quad ,$$

$$\tau^T_{ETF}(\vec{r}) = \frac{1}{2\pi^2}\left(\frac{2m^*}{\hbar^2}\right)^{5/2} \{T^{5/2} J_{3/2}(\eta) - \tag{4.10}$$
$$- \frac{1}{4}\frac{\hbar^2}{2m^*}\left[\frac{3}{8}T^{-1/2} J_{-3/2}(\eta)(\vec{\nabla}V)^2 + \frac{5}{6}T^{1/2} J_{-1/2}(\eta)\Delta V\right]\} \quad ,$$

$$\sigma_{ETF}(\vec{r}) = \frac{1}{2\pi^2}\left(\frac{2m^*}{\hbar^2}\right)^{3/2} T^{3/2}\left\{\frac{5}{3} J_{3/2}(\eta) - \eta J_{1/2}(\eta) + \right. \tag{4.11}$$
$$\left. + \frac{1}{24}\frac{\hbar^2}{2m^*}\left[\frac{1}{4}T^{-3} J_{-3/2}(\eta)(\vec{\nabla}V)^2 - T^{-2} J_{-1/2}(\eta)\Delta V\right]\right\} \quad ,$$

$$\eta = \frac{\lambda - V(\vec{r})}{T} \tag{4.12}$$

and $J_\nu(\eta)$ are the Fermi integrals

$$J_\nu(\eta) = \int_0^\infty \frac{x^\nu}{1 + \exp(x-\eta)}\, dx \quad . \tag{4.13}$$

To lowest order in eqs. (4.9) - (4.11) we recognize the well-known TF expressions. At this order it is possible to eliminate the quantity η numerically from the above densities; this defines the exact TF functionals at T > 0:

$$\tau^{T>0}_{TF}[\rho] = \tau_{TF}[\eta(\rho)] \quad , \tag{4.14}$$

$$\sigma_{TF}[\rho] = \sigma_{TF}[\eta(\rho)] \quad , \tag{4.15}$$

where $\eta(\rho)$ is obtained from inverting the function $J_{1/2}(\eta)$ in the leading (TF) term of eq. (4.9). Unfortunately, this procedure cannot be extended in an obvious way to include correctly all the $\hbar^2$-corrections. We are thus forced to make further approximations. Two possible ways shall be discussed in the following.

4.2.a) Low temperature expansion

In the limit $\eta>>1$, i.e. for $T<<(\lambda - V)$, the Fermi integrals can be expanded in a series of decreasing powers of η [85]

$$J_\nu(\eta) = \frac{\eta^{\nu+1}}{\nu+1}\left[1 + \nu(\nu+1)\frac{\pi^2}{6}\eta^{-2} + \dots\right] \quad . \tag{4.16}$$

The leading terms of the $J_\nu(\eta)$ give then just the old expressions $\rho_{ETF}(\vec{r})$ and $\tau_{ETF}(\vec{r})$ at $T = 0$, eqs. (2.26), (2.27); the next terms give corrections of order T^2. From these expressions one obtains the corrected functionals:

$$\tau^T_{ETF}[\rho] = \tau_{ETF}[\rho] + \frac{2m^*}{\hbar^2}\alpha(\rho)T^2, \tag{4.17}$$

$$\sigma_{ETF}[\rho] = 2\alpha(\rho)T \quad , \tag{4.18}$$

where

$$\alpha(\rho) = \frac{1}{12}(3\pi^2)^{1/3}\left(\frac{2m^*}{\hbar^2}\right)\rho^{1/3} \quad . \tag{4.19}$$

As in the $T = 0$ case, higher order corrections would contain inverse powers of ρ and must therefore be left out.

The total free energy density then becomes

$$\mathcal{F}(\vec{r}) = \mathcal{F}[\rho] = \mathcal{E}[\rho] - \alpha(\rho)T^2, \tag{4.20}$$

where $\varepsilon[\rho]$ is the full ETF energy density functional described in sect. 2 for $T = 0$. Note that the spatial integral of $\alpha(\rho)$ is nothing but the TF approximation to the well-known level density parameter a_0

$$a_0 = \frac{\pi^2}{6}\tilde{g}(\lambda) \quad , \tag{4.21}$$

where $\tilde{g}(\lambda)$ is the average single-particle level density (of one kind of particles). The functional eqs. (4.19), (4.20) has been used by several autors[86,87] to discuss thermal properties of nuclei. In the case of a variable effective mass $m^*(\vec{r}) = m/f(\vec{r})$, two correction terms to eq. (4.19) arise which remain finite; they have been shown, however, not to modify the numerical results very much.[15]

The problem with the above relations is that the low-temperature expansion $T << (\lambda - V)$ is only justified in the interior part of the nucleus (or in infinite nuclear matter), where $\lambda - V$ is of the order

of 30 - 40 MeV and the approximation holds up to fairly high temperatures. In the nuclear surface, however, λ-V quickly becomes smaller, going through zero at the classical turning points which still are in the surface region where the density is a few percent of its saturation value. Thus in the very region where one is interested in going beyond the TF approximation, namely in the surface region, the low-T expansion breaks down. It is thus not surprising that unsatisfactory results have been obtained with the functional (4.20).[88,89]

4.2.b) Gradient-corrected finite T functional

Since the low-T expansion breaks down in the surface, one might try to use the exact relations (valid for all T) at least in the TF approximation given above, and to add the gradient correction terms $\tau_2[\rho]$ and $\tau_4[\rho]$ known from the T = 0 case in an ad hoc manner. This leads to the functional

$$\tau_{ETF*}[\rho] = \tau_{TF}^{T>0}[\rho] + \tau_2[\rho] + \tau_4[\rho] \qquad (4.22)$$

where $\tau_{TF}^{T>0}[\rho]$ is the exact finite T functional in eq. (4.14). Since we cannot know any gradient corrections to $\sigma[\rho]$ at T = 0 we will use $\sigma_{TF}[\rho]$ eq. (4.15) along with $\tau_{ETF*}[\rho]$. This procedure has been proposed by Barranco and Treiner[88,89]; they used, however, a readjusted Weizsäcker term in $\tau_2[\rho]$ and omitted $\tau_4[\rho]$ which, as we have seen in sect. 3, is to be used very cautiously.

4.2.c) Comparison of numerical results

We shall in the following be using both approximate ETF functionals, eqs. (4.20) and (4.22), including in all cases the full, unrenormalized "cold" correction terms $\tau_2[\rho]$, $\tau_4[\rho]$, as well as $\tilde{J}_2[\rho]$ and $\tilde{J}_4[\rho]$ discussed in sect. 2. We also shall quote results obtained with the partial resummation method described in sect. 4.1 which can be generalized to finite temperatures without difficulties.[74,84] In fact, for that purpose it is sufficient to replace the exact Bloch density C in eq. (4.7) by that obtained with the partial resummation method. Since the Laplace inversion there is made numerically by the saddle point method, it causes no problem to take into account the temperature dependent factor in eq. (4.7) exactly (i.e. without low-T expansion). We shall first test the different approximations using the force SIII for which HF calculations at T > 0 have been performed[79] and can be used for comparison.

In figure 9 we plot for ^{208}Pb the "effective level density parameter" a_{eff} defined by

$$a_{eff} = \frac{S^2}{4E^*} \qquad (4.23)$$

versus the excitation energy E*

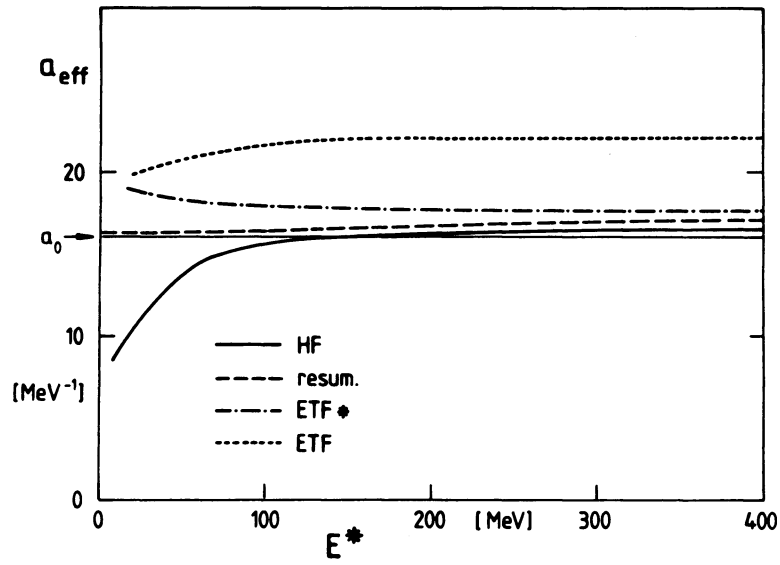

Fig. 8. Effective level density parameter a_{eff} eq. (4.23) for ^{208}Pb versus excitation energy E* for ^{208}Pb (SIII force used). The various approximations are: HF (full line), partial resummation method (dashed line), modified ETF* functional with exact T dependence in the TF terms, eq. (4.22) (dashed-dotted line), and low-T-expanded ETF functional eq. (4.20) (dotted line). a_0 is the level density parameter eq. (4.21).

$$E^* = E(T) - E(0). \tag{4.24}$$

The relation (4.23) is that of the Fermi gas theory which is reached when the shell effects are washed out,[79] so that in this limit a_{eff} tends to the level density parameter a_0 defined in eq. (4.21). We see in fig. 8, indeed, that the curves $a_{eff}(T)$ are approximately constant for $E^* \gtrsim 150$ MeV (corresponding to $T \gtrsim 3$ MeV).

Whereas the HF result approaches the correct value a_0 eq. (4.21) - for the slight variation at $E^* \gtrsim 200$ MeV see the discussion in ref. 79 - , the low-T expanded functional (ETF) leads to a value which is more than 30 % too high. This is the well-known failure of this approximation.[89] The modified functional eq. (4.22) (ETF*) gives an asymptotic value of a_{eff} only ~ 7 % higher than the HF result, which is a considerable improvement. The result of the partial resummation method, in which the temperature dependence is treated exactly, comes closest to the HF result and clearly is an excellent

approximation above $E^* \simeq 100$ MeV where the shell effects have disappeared.

In refs. 15,84 it was also shown that the temperature dependence of the r.m.s. radii obtained with HF is very well reproduced by both the ETF* functional eq. (4.22) and the resummation method, whereas with the low-T expanded functional eq. (4.20) it is strongly exaggerated above $T \simeq 3$ MeV.

A question which has been much discussed in the literature is how the fission barriers depend on temperature.[81,86,87,90] The fission of an excited nucleus is usually thought to be an isothermal process; therefore one has to look at the deformation behavior of the free energy F. Due to the well-known decrease of the free surface energy, the fission barriers also decrease with increasing temperature. (The variation of the Coulomb energy with temperature is not very important.) This was shown by explicit calculations of fission barriers with the variational ETF method at $T > 0$.[15]

In table 5 we list as a function of temperature the free surface energy a_s^∞ obtained with the three above methods for the SkM* force. It is clearly seen that the low-T expansion leads to an exaggeration

Table 5

T	a_s^∞ ETF	a_s^∞ ETF*	a_s^∞ resum.	ETF* a_c^*	ETF* Q	ETF* k_s	J
0	17.51	17.51	17.63	10.3	35.4	-57.3	30.03
1	17.30	17.33	17.53	10.0	35.3	-57.4	30.00
2	16.64	16.85	17.22	9.6	35.0	-57.5	29.91
3	15.50	16.08	16.70	8.7	34.4	-57.9	29.76
4	13.78	15.08	15.70	7.7	33.5	-58.6	29.54

LDM and droplet model parameters (all in MeV) for the force SkM* as functions of temperature T (in MeV). The free surface energy a_s^∞ is obtained in three approximations discussed in the text; the parameters a_c^*, Q and k_s are obtained with the ETF* functional eq. (4.22). For the volume asymmetry energy J, all approximations give the same result.

of the temperature dependence of a_s^∞. The partial resummation method (3rd column) reproduces the T-dependence found in HF calculations at $T \gtrsim 2$ MeV; the corrected functional $\tau_{ETF}^*[\rho]$ eq. (4.22) comes rather close to it, althoug the decrease of a_s^∞ with T here also is somewhat too strong. We also give in table 5 the effective curvature energy a_c^* eq. (3.28), the surface stiffness parameter Q and the surface asymmetry energy k_s defined by[15,54]

$$K_s = -\frac{9}{4}\frac{J^2}{Q} \,, \tag{4.25}$$

all evaluated for semi-infinite nuclear matter with Fermi function profiles. It is interesting to note that the absolute value of k_s increases with T due to the inverse dependence of Q which decreases faster with T than the volume asymmetry energy J (given in the last column of tab. 5).

We learn from these results that the temperature dependence of surface properties depend rather crucially on the approximations made. In particular, the low-T expansion leads to rather bad results which strongly exaggerate the T dependence. The best agreement with finite-T HF results is obtained with the partial resummation method, and reasonable agreement with the corrected ETF* functional eq. (4.22) in which the exact T dependence is contained in the TF expressions for $\tau[\rho]$ and $\sigma[\rho]$. In the context of density functional theory there remains, however, still a challenge to find better functionals $\tau[\rho]$ and $\sigma[\rho]$ in which the correct T dependence is contained also in the gradient corrections.

4.3. Application of the ETF Method to the Nuclear Breathing Mode [68]

We finally want to mention briefly an application of the variational ETF method to the calculation of the nuclear breathing mode energies.[68] We refer to the lectures of Holzwarth[91] and Treiner[92] for detailed discussions of the nuclear giant resonances of which the breathing mode, corresponding to density compressional vibrations, has only recently been established experimentally.

Starting from spherical nuclear ground-state densities described by simple Fermi functions, we can introduce compression modes by writing

$$\rho_q(r,t) = \frac{\rho_{0q}^c(t)}{1+\exp\left(\frac{r-R_q^c(t)}{\alpha_q^c(t)}\right)} \,, \tag{4.26}$$

where the density parameters now are supposed to be periodically time dependent functions:

$$\rho_{0q}^c(t) = \rho_{0q} + \delta\rho_{0q}\sin(\omega t) \,, \tag{4.27}$$

etc. We shall define two independent dimensionless (isoscalar) collective degrees of freedom by

$$q_\rho(t) = \frac{\rho_{0q}^c(t)}{\rho_{0q}} = 1 + \delta q_\rho(t) \,, \tag{4.28}$$

$$q_\alpha(t) = \frac{\alpha_q^c(t)}{\alpha_q} = 1 + \delta q_\alpha(t) \; ; \qquad (4.29)$$

the radii parameters $R_q^c(t)$ shall for each set of values q_ρ, q_α be determined by the conservation of particle numbers. The variables q_ρ and q_α define a two-dimensional collective Hamiltonian ($i,j = \rho,\alpha$)

$$H_{coll} = \frac{1}{2}\sum_{i,j} B_{ij}\,\dot{q}_i\,\dot{q}_j + \frac{1}{2}\sum_{i,j} K_{ij}\,(q_i - 1)(q_j - 1) + E_0 \; ; \qquad (4.30)$$

we have assumed small amplitude oscillations ($\delta q_i \ll 1$) and therefore used a quadratic approximation of the potential energy part. The compressibility modulus K_{ij} can easily be determined[68] from the variational ETF ground-state energies discussed in sect. 3.2, by

$$K_{ij} = 9\,\frac{\partial^2}{\partial q_i \partial q_j}\left(\frac{E}{A}\right) \; ; \qquad (4.31)$$

shell effects in the K_{ij} are small (of the order of ~ 1 %) and can therefore be safely neglected. The inertial tensor B_{ij} can be obtained from classical hydrodynamics (which is allowed for the 0^+ mode[91]) in terms of the velocity fields $v_i(r)$:

$$B_{ij} = \frac{9}{A}\,m\int \rho\, v_i\, v_j\, d^3r \; ; \qquad (4.32)$$

the latter can be found from solving the continuity equations

$$\frac{\partial \rho}{\partial q_i} + \vec{\nabla}\cdot(\rho\,\vec{v}_i) = 0 \; ; \qquad \vec{v}_i(r) = \frac{\vec{r}}{r}\,v_i(r) \qquad (4.33)$$

(here $\rho = \rho_n + \rho_p$). Eq. (4.30) is that of two coupled harmonic oscillators (taking B_{ij} to be constant at $q_i = 1$); it is solved by diagonalizing the secular matrix $K_{ij} - \omega^2 B_{ij}$. Of the two resulting frequencies ω_1, ω_2 we can identify the lower with the experimentally known breathing mode energy

$$\hbar\omega_1 = E_{0^+} = E_{GMR} \; ; \qquad (4.34)$$

the second corresponds to a higher mode (still to be found).

In figure 9 we show the results of the semiclassical calculations obtained in this way with the SkM* force; they are seen to reproduce perfectly the experimental peak energies within their error bars.

This result illustrates, as an example, the usefulness of the variational ETF approach also in dynamical applications. In fact, the breathing mode energies shown in fig. 9 are practically identi-

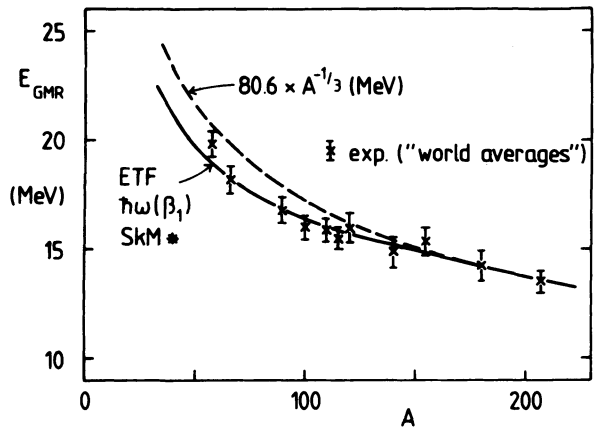

Fig. 9. Breathing mode (giant monopole resonance, GMR) energies versus nucleon number. Crosses are experimental peak energies with error bars, taken from ref. 36. The solid line shows the energies $\hbar\omega(\beta_1) = \hbar\omega_1$ found from the ETF model calculations[68] with the SkM* force.

cal with those which are obtained in microscopical RPA calculations at much higher cost. Furthermore, the interpretation in terms of oscillating parameters of simple trial densities gives a rather nice physical insight into the role of the couplings of surface and bulk contributions to the breathing mode.[68]

5. ACKNOWLEDGEMENTS

The author is indebted to C. Guet and H.-B. Håkansson, with whom most of the ETF calculations were performed in a fruitful collaboration, and to J. Bartel and W. Stocker for their contributions to the work discussed in the last section.

Note added in proof:

The correct functionals $\tau[\rho]$ and $\sigma[\rho]$ up to second order with temperature-dependent coefficients have meanwhile been derived in ref.[93].

REFERENCES

1. C.F. v. Weizsäcker, Z. Phys. 96: 431 (1935)
2. H.A. Bethe and F. Bacher, Rev. Mod. Phys. 8: 82 (1936)
3. T.H.R.Skyrme, Phil. Mag. 1: 1043 (1956); Nucl. Phys. 9: 615 (1959)
4. R.A. Berg and L. Wilets, Phys. Rev. 101: 201 (1956); L. Wilets, Rev. Mod. Phys. 30: 542 (1958)
5. K. Kumar and R.K. Bhaduri, Phys. Rev. 122: 1926 (1961)
6. K.A. Brückner, J.R. Buchler, S. Jorna and R.L. Lombard, Phys. Rev. 171: 1188 (1968); H.A. Bethe, Phys. Rev. 167: 879 (1973)
7. R.J. Lombard, Ann. of Phys. 77: 380 (1973)
8. J.P. Hohenberg and W. Kohn, Phys. Rev. 136: B 864 (1964)
9. G.E. Brown and A.D. Jackson, The Nucleon-Nucleon-Interaction (North-Holland/Amer. Elsevier, New York, 1976)
10. K.A. Brückner, Phys. Rev. 97: 1353 (1955)
11. K.A. Brückner, J.L. Gammel and H. Weitzner, Phys. Rev. 110: 431 (1958)
12. H.A. Bethe, Ann. Rev. Nucl. Sci. 21: 93 (1972)
13. J.W. Negele, Phys. Rev. C1: 1260 (1970); J.W. Negele and D. Vautherin, Phys. Rev. C5: 1472 (1972); C11: 1031 (1975)
14. C. Guet, H.-B. Håkansson and M. Brack, Phys. Lett. 97 B: 7 (1980)
15. M. Brack, C. Guet and H.-B. Håkansson, Regensburg Preprint TPR-83-16, submitted to Physics Reports
16. J. Bartel, P. Quentin, M. Brack, C. Guet and H.-B. Håkansson, Nucl. Phys. A 386: 79 (1982)
17. O. Bohigas, A.M. Lane and J. Martorell, Phys. Reports 51: 267 Phys. Reports 51: 267 (1979)
18. J.P. Blaizot, Phys. Reports 64: 171 (1980)
19. P. Quentin and H. Flocard, Ann.Rev.Nucl.Part.Sci. 28: 523 (1978)
20. D. Vautherin and D.M. Brink, Phys. Rev. C 5: 626 (1972)
21. V.M. Strutinsky, Nucl. Phys. A 95: 420 (1967); A 122: 1 (1968)
22. M. Brack, J. Damgård, A.S. Jensen, H.C. Pauli, V.M. Strutinsky and C.Y. Wong, Rev. Mod. Phys. 44: 320 (1972)
23. M. Brack and P. Quentin, Nucl. Phys. A 361: 35 (1981)
24. E.P. Wigner, Phys. Rev. 40: 749 (1932); J. G. Kirkwood, Phys. Rev. 44: 31 (1933)
25. R.K. Bhaduri and C.K. Ross, Phys. Rev. Lett. 27: 606 (1971)
26. B.K. Jennings, Nucl. Phys. A 207: 538 (1973)
27. B.K. Jennings, R.K. Bhaduri and M. Brack, Nucl. Phys. A 253: 29 (1975) and references quoted therein
28. M. Brack and H.C. Pauli, Nucl. Phys. A 207: 401 (1973)
29. M. Brack, B.K. Jennings and Y.H. Chu, Phys. Lett. 65 B: 1 (1976)
30. B. Grammaticos and A. Voros, Ann. of Phys. 123: 359 (1979); 129: 153 (1980)
31. C. Guet and M. Brack, Z. Phys. A 297: 247 (1980)
32. D. Vautherin, Phys. Rev. C 7: 296 (1973)
33. C. Titin-Schnaider and P. Quentin, Phys. Lett. 49 B: 397 (1974)

34. M.J. Giannoni and P. Quentin, Phys. Rev. C 21: 2076 (1980)
35. M. Beiner, H. Flocard, N.V. Giai and P. Quentin, Nucl. Phys. A 238: 29 (1975)
36. J. Treiner, H. Krivine, O. Bohigas and J. Martorell, Nucl. Phys. A 371: 253 (1981)
37. F. Tondeur, Phys. Lett. 123 B: 139 (1983); F. Tondeur, M. Brack, M. Farine and J.M. Pearson, Preprint 1983
38. W. Kohn and L.J. Sham, Phys. Rev. 137: A 1697 (1965); 140: A 1133 (1965)
39. R. Balian and C. Bloch, Ann. of Phys. 69: 76 (1972) and earlier references quoted therein
40. V.M. Strutinsky, A.G. Magner, S.R. Ofengenden and T. Døssing, Z. Phys. A 283: 269 (1977)
41. A.S. Tyapin. Sov. J. Nucl. Phys. 11: 401 (1970); 14: 50 (1972)
42. G.E. Uhlenbeck and E. Beth, Physica 3: 729 (1936)
43. B.K. Jennings, Ph. D. Thesis, McMaster University, 1976 (unpublished)
44. A. Voros, Thèse d'Etat, Paris University, Orsay, 1977 (unpublished)
45. N.L. Balazs and B.K. Jennings, preprint TRI-PP-83-55, 1983, to be published in Physics Reports
46. H. Krivine and J. Treiner, Phys. Lett. 88 B: 212 (1979)
47. X. Campi and S. Stringari, Nucl. Phys. A 337: 313 (1980)
48. J. Treiner and H. Krivine, Preprint Orsay IPNO/TH 82-18, 1982.
49. W. Stocker, G. Süssmann and S. Knaak, Nucl. Phys. A 187: 38 (1972)
50. O. Bohigas, X. Campi, H. Krivine and J. Treiner, Phys. Lett. 64 B: 381 (1979)
51. H. Krivine, J. Treiner and O. Bohigas, Nucl. Phys. A 366: 155 (1980)
52. E. Lieb, Rev. Mod. Phys. 53: 603 (1981)
53. V.M. Strutinsky and A.S. Tyapin. Sov. Phys. JETP 18: 664 (1964)
54. W.D. Myers and W.J. Swiatecki, Ann. of Phys. 55: 395 (1969); 84: 186 (1974)
55. Y.H. Chu, B.K. Jennings and M. Brack, Phys. Lett. 68 B :407 (1977); see also Y.H. Chu, Ph.D. Thesis, Stony Brook 1977, unpubl.
56. C.M. Ko, H.C. Pauli, M. Brack and G.E. Brown, Nucl. Phys. A 236: 269 (1974)
57. M. Brack, Phys. Lett. 81 B: 239 (1977)
58. J.B. Bellicard et al., Saclay progress report CEA-N-2207: 81 (1981)
59. S. Köhler, Nucl. Phys. A 258: 301 (1976)
60. H. Flocard, P. Quentin, A.K. Kerman and D. Vautherin, Nucl. Phys. A 203: 433 (1973)
61. D. Gogny, Nucl. Phys. A 237: 399 (1975)
62. M. Brack, in "Physics and Chemistry of Fission 1979", Jülich (IAEA Vienna, 1980) Vol. I, p. 227
63. W.D. Myers and W.J. Swiatecki, Nucl. Phys. 81: 1 (1966)
64. M. Brack, C. Guet, H.-B. Håkansson, A. Magner and V.M. Strutinsky, 4th Int. Conf. on nuclei far from stability,

Helsingør 1981 (CERN 81-09, Geneva) p. 65
65. M. Farine, J. Côté and J.M. Pearson, Phys. Rev. C 24: 303 (1981), and earlier references therein
66. M. Pearson, Nucl. Phys. A 376: 507 (1982)
67. F. Tondeur, J.M. Pearson and M. Farine, Nucl. Phys. A 394: 462 (1983)
68. M. Brack and W. Stocker, Nucl. Phys. A 388: 230 (1982); A 406: 413 (1983)
69. F. Tondeur, Nucl. Phys. A 315: 353 (1978)
70. R.K. Bhaduri, Phys. Rev. Lett. 39: 329 (1977)
71. M. Durand, M. Brack and P. Schuck, Z. Phys. A 286: 381 (1978); A 296: 87 (1980)
72. J. Bartel, M. Durand and M. Brack, Z. Phys. A 315: 341 (1984);
73. J. Bartel and M. Vallieres, Phys. Lett. 114 B: 303 (1982)
74. J. Bartel, PhD Thesis, University of Regensburg, 1984; and to be published
75. M. Lefort, Nucl. Phys. A 387: 3c (1982), and references quoted therein
76. see, e.g. J.M. Lattimer, Ann. Rev. Nucl. Part. Sci. 31: 337 (1981), and references quoted therein
77. P. Bonche and D. Vautherin, Nucl. Phys. A 372: 496 (1981); Astron. Astrophys. 112: 168 (1982)
78. see, e.g. J. Des Cloiseaux in "Many Body Physics", Les Houches 1967 (Gordon and Breach, New York, 1968) p. 1
79. M. Brack and P. Quentin, Phys. Lett. 52 B: 159 (1974); Physica Scripta A 10: 163 (1974); see also ref. 23
80. U. Mosel, P. Zint and K.H. Passler, Nucl. Phys. A 236: 252 (1974)
81. G. Sauer, H. Chandra and U. Mosel, Nucl. Phys. A 264: 221 (1976)
82. M. Barranco and J.R. Buchler, Phys. Rev. C 22: 1729 (1980); C 24: 1191 (1981);
D.Q. Lamb, J.M. Lattimer, C.J. Pethick and D.G. Ravenhall, Nucl. Phys. A 360: 459 (1981)
83. D.G. Ravenhall, C.J. Pethick and J.M. Lattimer, Nucl. Phys. A 407: 572 (1983)
84. J. Bartel, M. Brack and C. Guet, Phys. Lett. B, in print
85. see, e.g., E.C. Stoner, Phil. Mag. 28: 257 (1939)
86. X. Campi and S. Stringari, Z. Phys. A 309: 239(1983)
87. M. Barranco, M. Pi and X. Viñas, Phys. Lett. 124 B: 131 (1983), and references quoted therein
88. M. Barranco and J. Treiner, Nucl. Phys. A 351: 269 (1981)
89. J. Treiner, preprint Orsay IPNO/TH 83-26
90. W. Stocker and J. Burzlaff, Nucl. Phys. A 202: 265 (1973); R.W. Hasse and W. Stocker, Phys. Lett. 44 B: 26 (1973)
91. G. Holzwarth, these proceedings
92. J. Treiner, these proceedings
93. M. Brack, Workshop on semiclassical methods in nuclear physics, Grenoble, 1984, to be published in Journal de Physique (Paris).